Bipolar Membrane and Interface Materials for Electrochemical Energy Systems

Tufa, Ramato Ashu; Blommaert, Marijn A.; Chanda, Debabrata; Li, Qingfeng; Vermaas, David A.; Aili, David

DOI
10.1021/acsaem.1c01140

Publication date
2021

Document Version
Accepted author manuscript

Published in
ACS Applied Energy Materials

Bipolar membrane and interface materials for electrochemical energy systems

Ramato Ashu Tufa[1,*], Marijn A. Blommaert[2], Debabrata Chanda[3], Qingfeng Li[1], David A. Vermaas[2,*], David Aili[1,*]

[1]*Department of Energy Conversion and Storage, Technical University of Denmark, Building 310, 2800 Kgs. Lyngby, Denmark*

[2]*Department of Chemical Engineering, Delft University of Technology, 2629 HZ Delft, The Netherlands*

[3]*Henan Key Laboratory of Polyoxometalate Chemistry, Henan Engineering Research Center of Resource & Energy Recovery from Waste, College of Chemistry and Chemical, Engineering, Henan University, Kaifeng 47504, PR China*

Corresponding authors:

*E-mail: rastu@dtu.dk (Ramato Ashu Tufa)

D.A.Vermaas@tudelft.nl (David Vermaas)

larda@dtu.dk (David Aili)

Abstract

Bipolar membranes (BPMs) are recently emerging as a promising material for application in advanced electrochemical energy systems such as (photo)electrochemical CO_2 reduction and water splitting. BPMs exhibit a unique property to accelerate water dissociation and ionic separation that allows for maintaining a steady-state pH gradient in electrochemical devices without a significant loss in process efficiency, thereby allowing a broader catalyst materials selection for the respective oxidation and reduction reactions. However, the formation of high performance BPMs with significantly reduced overpotentials for driving water dissociation and ionic separation at conditions and rates that are relevant to energy technologies is a key challenge. Herein, we perform a detailed assessment of the requirements in base materials and optimal design routes for the BPM layer and interface formation. In particular, the interface in the BPM presents a critical component with its structure and morphology influencing the kinetics of water dissociation reaction governed by both electric field and catalyst driven mechanisms. For this purpose, we present, among others, the advantages and drawbacks in the utilization of a bulk heterojunction formed in 3D structures that recently have been reported to demonstrate a possibility of designing stable and high performance BPMs. Also, the outer layers of a BPM play a crucial role in kinetics and mass transport, particularly related to water and ion transport at electrolyte-membrane and membrane-catalyst interfaces. This work aims at identifying the gaps in the structure-property of the current monopolar materials to provide prospective facile design routes for BPMs with excellent water dissociation and ionic separation efficiency. It extends to a discussion about material selection and design strategies of advanced BPMs for application in emerging electrochemical energy systems.

KEYWORDS: Ion exchange membrane, bipolar membrane, water dissociation, pH gradient, 2D/3D interfaces, energy conversion and storage

1. Introduction

Advancing renewable energy technologies for efficient storage and utilization at a large scale is a crucial strategy to create a carbon-neutral economy.[1] In recent years, the cost of renewables such as solar and wind is reducing significantly and call for optimal technologies toward large-scale energy storage. In this regard, electrocatalytic fuel and chemical production is one promising approach. For instance, energy can be stored in hydrogen formed by the electrolysis of water, which can later be converted to electricity e.g. in fuel cells by the reaction of hydrogen and oxygen. Electrochemical CO_2 reduction also offers an advantage of seasonal renewable electricity storage in the form of various carbon-based products (chemicals and fuels) depending on the employed electrocatalysts and reaction conditions. However, the practical applicability of such systems as large-scale technological solutions is still limited in many ways.

In visions associated with hydrogen as an energy carrier or electrochemical CO_2 reduction, water has involved in the electrode reactions, for example, the electrolysis of water to hydrogen or the co-electrolysis of water and CO_2 to value-added fuels and chemicals. In a typical water electrolyzer, the hydrogen-evolution reaction at the cathode and oxygen-evolution reaction at the anode are facilitated by the use of catalysts that have different requirements of reaction conditions depending on the employed system. Platinum (Pt)-group-based electrocatalysts for the hydrogen-evolution reaction effectively work in highly acidic reaction conditions: the exchange current density for Pt at pH 0 is about 100 times higher than the exchange at pH 14.[2] On the other hand, earth-abundant electrocatalysts such as Fe and Ni are sufficiently active towards the oxygen-evolution reaction but must be utilized in an alkaline medium due to the restricted stability.[3] In electrochemical cells, a cation-exchange membrane (CEM) like Nafion® is used in strongly acidic electrolytes whereas an anion-exchange membrane (AEM) such as Sustanion® is typically used

in strongly alkaline electrolytes. The challenge here comes when using the same electrolyte (same pH) on both the anode and cathode sides, which brings up stability and compatibility issues of the employed electrocatalysts. In electrochemical CO_2 reduction, the pH at the cathode is preferably maintained at near-neutral pH to avoid the competing hydrogen-evolution reaction at low pH whereas the anode is maintained at pH 14. Any pH gradients between the flowing catholyte and anolyte layers are practically unfeasible due to the gradual intermixing and acid-base neutralization at the interface. This becomes possible with BPMs where the negatively charged acidic groups are fixed to the CEM matrix and the positively charged basic sites are fixed to the AEM matrix. Therefore, an integrated system coupling a CEMs and an AEMs are viable to operate with distinct electrolyte layers at each side along with the compatible electrocatalysts.

In recent days, BPMs have emerged as promising solutions to overcome some of the challenges associated with monopolar membranes for applications in electrochemical energy systems[4]. A BPM consists of polymeric CEM and AEM conjoined together by an active interface between the membranes where a chemical process e.g. dissociation or association of the two active charge carriers, H^+ and OH^- from/into water occurs. The separation of the acidic and alkaline electrolytes layers with an interfacial junction opens the possibility to operate the two half-reactions at different pH values, which significantly broadens the scope of catalyst materials that combine high activity, good stability, and natural abundance.[5] The structure of electrolyte layers with the transport of distinct charge carriers has also been demonstrated to effectively reduce the cross-over issues in electrochemical CO_2 reduction either by mitigating the net transport of neutral or ionic products between the anodic and cathodic compartments or by reducing the parasitic CO_2 pumping, which is unavoidable in cells based on conventional electrolyte systems.

BPMs have been extensively used for the production of acids and bases in the electrodialysis (ED) process for many years,[6, 7] and more recently in other electrochemical systems such as water electrolyzers,[8, 9] fuel cells,[10, 11] flow batteries [12, 13] and electrochemical CO_2 reduction.[14-17] Based on the significant amount of experimental investigations reported in the literature, two review articles on BPM design aspects and applications have been recently published.[6, 7] Pärnamäe *et al*.[6] presented a comprehensive overview of the BPM development of last 70 years from fundamentals to membrane synthesis, properties and applications including resource recovery/regeneration, (waste) water treatment, food processing and energy-related aspects. The review by Giesbrecht *et al*. focuses on recent advances in material understanding, characterization methods particularly the construction and optimization of the interface layer[7]. The present work, biulding on these works, is devoted to a detailed assessment of the materials requirements and design aspects in association with electrochemical energy technologies, an emerging class of BPM applications such as water electrolysis, CO_2 reduction, batteries and fuel cells. Emphasis is placed on the most recent material developments for tuning properties of individual AELs and CELs along with the interfacial layer (IL) aiming at identifications of key scientific considerations and research gaps in material and design aspects towards advanced BPM development for applications in the emerging energy devices.

2. Theoretical Background

Ion transport and water dissociation in BPMs involve several multidisciplinary concepts. In principle, BPMs can be operated in two main configurations: the forward bias mode and reverse bias mode (Figure 1). In forward bias (Figure 1a), where the AEM faces the anode and CEM faces the cathode, the respective ions enter into the IEM layers and accumulate at the BPM interfacial layer (BPM-IL), which results in charge compensation of the layers and the permeation of co-ions

through IEM layers. The ions from either side of the membrane are transported to the IL where they react to form a product. Despite the existence of few demonstrations of this configuration in the literature on fuel cells [10] and batteries,[18-20] it is not well demonstrated for application in most common electrochemical devices.

Reverse bias mode is by far the most widely used configuration in various applications. Under reverse polarization (Figure 1b), the counterions are being pulled out of the interfacial layer under the influence of the applied voltage with coions from the solution largely excluded from entering the respective membrane layers. Thus, the absence of mobile ions at the IL results in a depleted electric double layer subsequently forming a thin space charge region (SCR) with a locally high electric field. Under this mode, ionic separation is observed at a sufficiently high cross-membrane potential, resulting in protons (H^+) and hydroxide (OH^-) ions which are driven towards the cathode and anode, respectively. The outward flux of protons and hydroxide ions promotes further water dissociation in line with Le Châteliers principle. This reaction is supposed to be driven by a different mechanism at the BPM interface which includes i) the catalytic proton transfer reaction between the water and the fixed groups and ii) the enhanced electric field effect defined by Onsager's theory of the second Wien effect.[21] Both Pärnamäe *et al*.[6] and Giesbrecht *et al*.[7] well presented the details on the mechanistic understanding of the water dissociation phenomenon at the BPM interface.

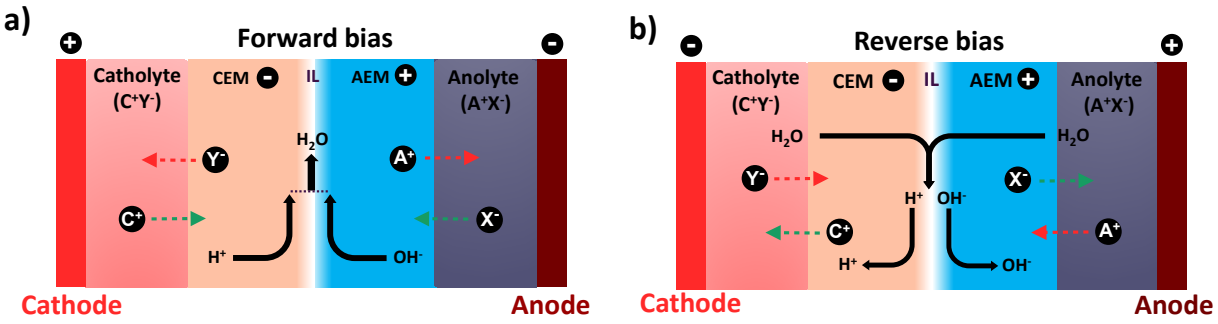

Figure 1. Bipolar membrane operation under a) forward and b) reverse-bias conditions. The direction of migration of ions due to the applied voltage is indicated by the green dashed arrows, whereas the direction for the migration of ions that are restricted by the membrane fixed charge groups is indicated by the red dashed arrows. A sufficient water supply at the BPM interface is needed to prevent dry out, facilitate a sustainable water dissociation and allow membrane operations at high current densities.

BPMs in contact with aqueous solution forms three main interfaces in electrochemical devices, namely the CEL-catholyte interface, the CEL-AEL interface (forming an IL depending on thickness), and the AEL-anolyte interface, which governs the potential difference over the BPM. Under zero current or open circuit conditions (OCV), the concentrations of the anions or cations in the membrane and solutions change depending on the diffusive flux and the nature and concentration of the fixed charge groups.[22] An electric field is created in a direction opposite to that of the diffusional flow of ions between the membranes and solutions, and a Donnan equilibrium is reached when the electric field balances the diffusional driving force of the ionic species (Figure 2a). This results in a Donnan potential across the different interfaces. Different potentials φ_1 , φ_2 and φ_3 representing the potential across the CEL-catholyte interface, the CEL-AEL interface and the AEL-anolyte interface, respectively, are recorded (Figure 2c). The potential over the BPM φ_{BPM} is obtained by summing up the aforementioned three potentials leading to:

$$\varphi_{BPM} = \frac{RT}{zF} \log \frac{\left[H^+_{An} \right]}{\left[H^+_{Ct} \right]} = 0.0591 \left(\mathrm{pH}_{An} - \mathrm{pH}_{Ct} \right) = 0.0591 \Delta \mathrm{pH} \quad (1)$$

The subscripts *Ct* and *An* represent the catholyte and anolyte, respectively. A rough assumption of about 1 meq g^{-1} of fixed charge density for classical IEMs implies that a concentration of about 1 M for H^+ in CEL and OH^- in AEL is required to balance the membrane fixed charge groups. Thus, under an extreme pH gradient (ΔpH = 14) across the membrane, φ_{BPM} reaches about 0.83 V (Eq. 3) representing the thermodynamic potential ($\varphi_{BPM,\min}$) required to maintain a pH difference of 14 across the BPM interface, which is generally in fair agreement with the practical values from experiments. Under the same condition, the Donnan potential difference across the membrane-electrolytes interfaces approaches zero. However, under a non-extreme pH gradient or at the concentrations of <1 M for H^+ and OH^- in the electrolytes, φ_{BPM} indicated a considerable deviation from these thermodynamic formulations [23, 24] attributed to the non-ideal behavior of membranes. [15, 24, 25]

When an external electric field is applied, an initial linear increase in electrical current vs. potential as in a typical I-V curve of the BPM is observed, which is attributed to migration of co-ions (Figure 2b). Details on the I-V behavior of the typical BPM is partly given in the supporting information (Figure S1) and the previous reviews on BPMs. [6, 7]

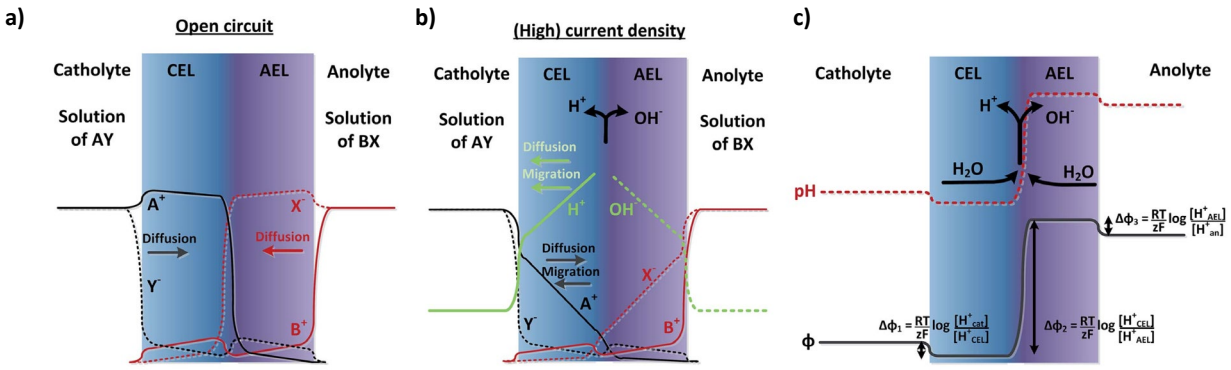

Figure 2. a) Concentration profiles of the electrolyte species at a thermodynamic equilibrium or open circuit voltage (OCV). Under OCV, the transport of ionic species in the respective membrane layers is governed by diffusion. b) Concentration profiles of the electrolytes species under steady-state current flow, and both diffusion and migration govern the transport of the ions. c) Potential and pH variations across a BPM at different interfaces depending on the activity of ions or pH. Under extreme pH conditions, the thermodynamic minimum of the potential required for water splitting is about 0.83 V, which varies depending on the nature (composition) of the interface, among others. Reproduced with permission. [25] Copyright 2018, Royal Society of Chemistry.

In BPM, water transport to/from the IL is mainly governed by the two phenomenons, either by concentration difference (osmosis) or the electroosmotic drag resulting in the outward flux of proton and hydroxide ions due to migration.[8] The amount of dragged H_2O is highly dependent on water uptake of the membrane, nature/composition of the membrane as well as the applied current density.[26] As such, the optimal design of BPMs in relation to the physical properties of the ionomer itself dependent on the water uptake and the fixed ion-exchange groups i.e. ion exchange capacity (IEC) of the membrane layers.[27] Although improved water uptake enhances the conductivity and membrane dry out in monopolar membranes, there are counteracting parameters in the case of BPMs. Besides the membrane dry out, low water uptake in BPM could result in the degradation of AEL by OH^- an attack on the functional groups.[28, 29] High water uptake in BPMs benefits in

terms of the prevention of membrane dry outs but this is associated with co-ion leakage. The water uptake properties of a BPM in relation to the water dissociation activity and stability are elaborated in the next section.

3. BPM properties as design criteria

Design criteria for a bipolar membrane (BPM) vary depending on the application of interest, among others. The required properties of the BPM also vary depending on the technology of interest. And the properties of the BPM depend on the inherent properties of its components (AEL, CEL, and IL), which also determines the cost and performance of the BPM. Figure 3 illustrates the interdependence of the different properties of the monopolar/BPM. Some of the key performance indicators determining membrane properties for BPMs are high water dissociation rate capability, low electrical resistance at high current densities (high ionic conductivity), high selectivity (low co-ion leakage or ion crossover) as well as good mechanical and chemical stability under the employed operating conditions.

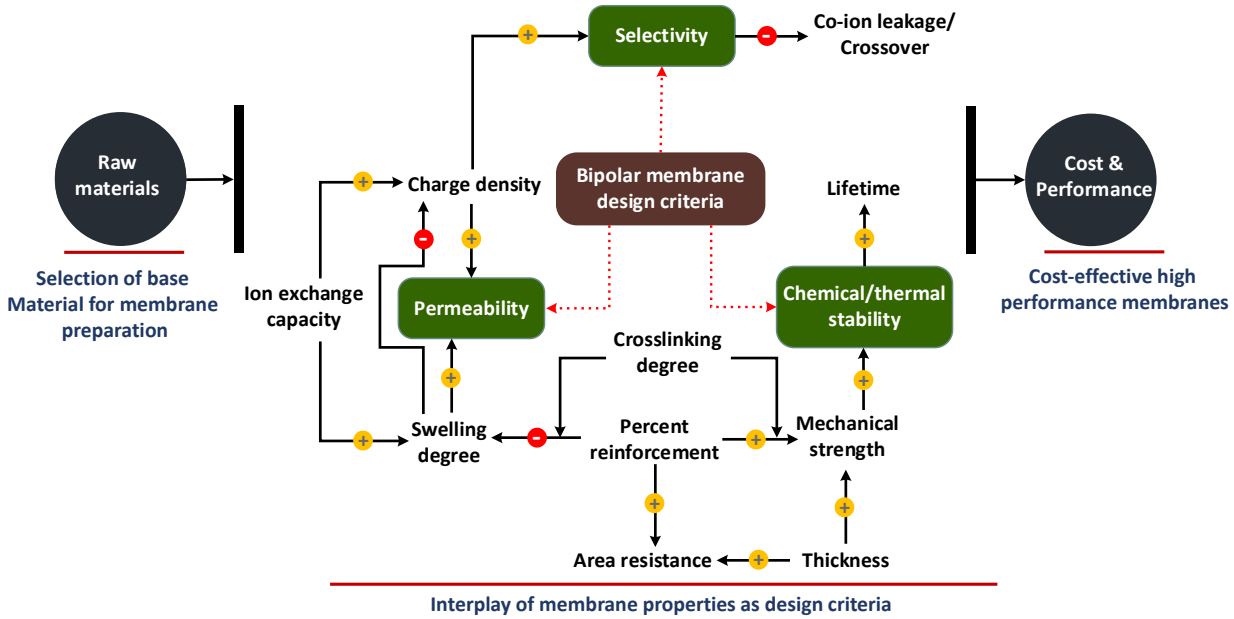

Figure 3. The interdependence of the monopolar and bipolar membrane properties: (+) signs indicate a positive impact and (-) signs indicate a negative impact on the respective membrane properties. Proper choice of the materials used for the monopolar layers, as well as the interfacial layers, highly determines the properties of the final BPM.

Water dissociation rate capability is by far the key parameter determining the performance of a BPM. Both the proton transfer reaction and electric field enhanced mechanistic routes for water dissociation are highly dependent on the structural and morphological properties of the BPMs, including the activity of the typically polymeric and/or inorganic catalysts utilized at the interface. In this regard, the nature of the functional groups in the membrane layers plays an important role. For instance, $–SO_3H$ has a lower rate constant (3×10^{-3} for the rate limiting proton transfer reaction) than that of $–N(CH_3)_3$ (0), and hence exhibits a higher catalytic activity for water dissociation.[30, 31] Experimental investigations on BPM interfaces tailored based on AEL containing quaternary ammonium (alkyl-substituted) functional groups displayed better performance than AELs based on bicyclic amines.[30] The enhanced water dissociation of the quaternary

ammonium(alkyl-substituted)-based AELs were claimed to be due to the catalytically active tertiary and secondary amines formed as a degradation product under a strong electric field in alkaline media. However, this is not a favorable condition from a stability point of view. Many other parameters also come into effect when tailoring the interface layer such as the water uptake and electrical conductivity of the interface layer. Such effects and other relevant phenomena at the BPM interface influencing the water dissociation efficiency are detailed in section 5.

3.1. Selectivity. A selective BPM should constitute membrane layers that minimize the crossover of co-ions from the supporting electrolytes into the bulk membrane layers. The selectivity in combination with the water dissociation in the IL allows for a continuous BPM operation in the presence of a pH gradient, which is not possible by using monopolar membranes. Practically, a small fraction of ions other than the water dissociation products (H^+ or OH^-) permeates through the BPM due to the non-ideal behavior of the membranes. This phenomenon of co-ion permeation or ion crossover of the BPM depends on several factors including the membrane microstructure (e.g. size of ion channel) and functionality as well as the concentration and composition of the electrolyte like pH and its species i.e. pH, activity, ion type (valence, size, and diffusion coefficient), etc, and the operating CD.[24, 25] For instance, a systematic study by Vermaas *et al*. on a series of electrolytes within a broad pH range under non-extreme condition ($\Delta pH < 14$) reveals that the contribution of the cations to the co-ion leakage (ion crossover) in BPM is larger than their corresponding salt anions for the same hydration radius.[24] Besides, highly concentrated electrolytes could result in the diffusion of more co-ions and/or counterions into the BPM bulk layers, cross-contamination, and hence amplification of current leakage.[32] Typical I-V behavior of a BPM indicates that the leakage current due to ion crossover and the water dissociation kinetics governs ion transport after a limiting current is reached at sufficiently large

applied voltages.[33] A more recent study elucidates the ion crossover driven by migration outweighs crossover due to diffusion for CD in the range of 10 - 40 mA cm^{-2}, and crossover due to migration becomes dominant at larger CDs.[25] Moreover, electrolytes with reduced ion crossover exhibit a reduced conductivity that would also impact the performance of BPM calling for complex membrane design strategies. Overall, selective BPM design with reduced ion-crossover enables the implementation of stable, high performance BPMs with limited electrolytes neutralization and a significant distortion of pH gradient.

3.2. Water uptake. The swelling property or water uptake of a BPM is important to maintain adequate water transport to the IL of BPM. A good swelling property benefits in terms of replenishment of the water consumed due to water dissociation at the IL. High permeability of the BPM layers for water molecules is related to the swelling property of the membranes that, in turn, influences both the membrane conductivity, selectivity and mechanical stability. It is well known that enhancing water uptake for monopolar membranes improves the membrane conductivity and reduces dry out but excessive water uptake may also lead to selectivity issues which is also a case more amplified in BPMs. Analysis based on model depictions indicates that an increase in water uptake depending on the salt ion transport coefficients in BPMs is highly associated with a significant increase of co-ion leakage (up to ~30 mA cm^{-2}).[27] However, modern BPM typically exhibits lower co-ion leakage lower than this (1-3 mA/cm^2). Highly swollen membranes are also prone to physical damage, particularly if the swelling ratio of the individual layers is different. Therefore, optimal trade-off values need to be considered for water uptake and conductivity membrane properties to design efficient BPM. From the design point of view, the swelling property of membranes is mostly optimized by controlling the degree of crosslinking in the membrane microstructure, but it is inevitable to avoid the associated increase in electrical

resistance. The conductivity of the membrane is mainly tuned by controlling the amount and nature of membrane functionalities, among others. Other parameters such as membrane thickness can also alter the membrane swelling behavior and hence the water transport properties.

3.3. Thickness. The thickness of the individual layers of a BPM influences the performance of the BPM in different ways, which has attracted research attention in recent years.[8, 34] Thicker and cross-linked layers provide more robust and selective IELs (reduced co-ion leakage), but increase the membrane resistance and hence voltage losses. The ohmic voltage losses due to resistance of the individual layers are, however, relatively small compared to the losses associated to driving the water dissociation and ionic separation under reversed bias operation.[4] The benefit of thick membranes in terms of selectivity needs to be controlled along with the membrane functionality or fixed charge density as these might alter the water transport properties. For this purpose, the use of asymmetric BPMs prepared by varying the thickness of one of the two membrane layers is one promising strategy to design BPM at a controlled selectivity and water transport properties.[35, 36] However, the challenge in such asymmetric BPM systems is the adhesion limitations resulting from the differences in the properties of the membrane layers, e.g. in terms of swelling behavior which may lead to delamination and mechanical failure [1]. Increasing the total BPM thickness by about 3-fold (from ~116 μm to 350 μm) resulted in about 7-fold reduction (from 700 mA cm^{-2} to 100 mA cm^{-2}) in water transport limited CD derived from the inflection of the I-V curves.[37] The state-of-art CD reported for a BPM with electrospun 3D (very thin morphology of ~ 45 μm junction) reaches up to ~1.1 A·cm^{-2} at a water dissociation overpotential of about ~0.6 V. Following a controlled thinning of AEM by electrode impregnation, a BPM-electrode assembly was developed for effective water splitting with a CD of up to 9 A cm^{-2} at a cell voltage of 2.2 V. Moreover, a recent study utilizing CEL as thin as 2 μm in combination with a 50 μm thick AEL

allowed reaching CD of up to 3.4 A cm^{-2} at a cell voltage of ~4 V in BPM electrolyzers.[34] Although the above works demonstrate the enhanced water transport property by thinning BPM layers, more research is required for a better correlation of thickness/thinness, water transport, co-ion leakage and the maximum CD.

3.4. Conductivity. The conductivity of the outer layers is characterized by good transport of ions within the membrane and at the proximity of the membrane interface. Particularly, fast transport of the water dissociation products (H^+ and OH^-) must be sustained for the realization of stable pH at each electrode. It is worth noting that the acid-base properties and hence the proton conductivity of the CEL could impact on the BPM performance in different ways. For example, a recent study demonstrated up to 40 % increase in faradaic efficiency for CO production during electrochemical CO_2 reduction utilizing a BPM CEL modified by weak acid polyelectrolyte layers following layer-by-layer assembly.[38] The authors hypothesized that the weak-acid CEL is associated with limited proton conduction from the IL due to lower local pH than its pK_a, results in relatively few free amine groups available for proton exchange. As such, limited proton transport to the cathode reduces the competing hydrogen evolution reaction at the cathode thereby enhancing the CO_2 reduction selectivity. However, there was no clarification of the possible impact of the layer-by-layer modification on the catalytic BPM water dissociation in relevance to the local pH requiring further study. High membrane conductivity or low resistance is also associated with an increase in the energy efficiency of electrochemical systems. Various strategies have been reported in the literature for improving membrane conductivity, which is detailed in sections 4.1 and 4.2, being more relevant to the IEC of the membranes. It is important to note here that an increase in IEC to enhance membrane conductivity might lead to excessive water uptake (swelling)

associated with a progressive dimensional loss, which requires a careful choice of base materials and functionalities.

3.5. Stability. The stability of the BPM is also a parameter worth considering as, for example, in strongly acidic and basic solutions, it determines the membrane lifetime. In BPM-based systems, the selectivity and stability of the CEL and AEL are very crucial for long-term operations with no delamination. The degradation in BPM-electrode assembly systems can be associated with the stability of the water dissociation catalysts at the interface. Blommaert *et al.* [39] used electrochemical impedance spectroscopy to investigate the degradation of BPM. Their results during the 5 days measurement indicated that the ohmic resistance increased by up to 10 % at OCV and 32% when applying current. Membrane degradation was also associated with an increase of both the water dissociation resistance and reduced conductivity of the outer layers. The performance losses were claimed to be associated with the reduced catalytic activity as well as the reduced fixed charge in the membrane due to an increase in the width of the IL. In general, during the long-term operation of electrochemical cells, there are possibilities of partial dissolution of the catalysts depending on the local pH variations spanning from the center of the interface to the membrane-electrolyte interface. A degradation mechanism for water dissociation catalyst based on NiO used in BPM-based water electrolyzer was hypothesized to be due to the dissolution of the NiO layer at a near-neutral pH environment within the interface as well as pH variations with the operating CDs.[34] This requires precise control and elucidation of the OH^- and H^+ concentration gradients at the BPM interface, to layout design perspectives for a stable BPM. Overall, properties that are generally relevant to the resistance or conductivity or selectivity are interdependent, which vary depending on IEC, water uptake, fixed charge density, etc. It is, therefore important to consider a careful choice of the base material and design strategies to combat the trade-off

challenges between the different properties and produce a high performance, low-cost BPM for the technology of interest.

4. Outer layer design requirements and materials

The outer layers of a BPM are the monopolar layers (CEL & AEL). These layers have two interfaces, one directed towards each other (IL, see further) and another that faces the adjacent electrolyte or catalyst. The properties of these monopolar layers, but also the interfaces between the BPM layers and the external environments or electrodes, and the interaction of the membrane with catalyst layers in membrane-electrode assemblies (MEAs) have a considerable impact on function and the mass transport in BPM devices.[7, 40] A wide range of membrane design and modification prospects are given in the literature for monopolar membranes that can be easily adapted for the design of BPMs.[41-43] A careful choice of the polymer backbone, as well as functionalities for the membrane layers, is crucial for designing BPMs with the optimal physicochemical and electrochemical properties for energy applications. Altering the local acidity/basicity of the BPM using functionalities with different pK_a of the outer layer and the BPM-electrode interface properties which influence the local electrode reaction could allow for the reduction of electrode overpotentials, particularly in zero-gap BPM devices.[32]

4.1. Cation exchange layer. An ideal CEL should facilitate the transport of cations while excluding anions, which is related to its selectivity. Besides the nature of the membrane, the properties of CEMs in a BPM are highly influenced by the composition of the support electrolyte and design strategies follow different principles depending on the specific property. For instance, selectivity can be tuned by surface modification techniques like forming a layer-by-layer surface film, surface cross-linking with the same functional groups as that of the membrane, forming a dense-neutral surface or surface layer with functional groups opposite to the membranes.[44-46]

Design strategies based on the preparation of the bulk membrane itself could involve the formation of pseudo-homogenous membranes, for example, by a combination of functionalized polystyrene and hydrophobic polymer through a block copolymer synthesis,[44, 47, 48] graft membranes based on the radical polymerization of styrene directly inside the hydrophobic film and hybrid membranes,[49-51] and composite membranes doped with inorganic particles.[52, 53]

Elucidation of the CEM structure and morphology with mobile species transport is one strategy towards the design of highly conductive CELs in BPMs. The nanomorphology of hydrated polymer electrolytes, particularly perfluorosulfonic acid membranes, has been intensively investigated.[54] It is a general understanding that many IEMs exhibit structural heterogeneity partitioning into hydrophilic channel domains and hydrophobic regions. Water transport and ionic conductivity of the bulk CEM materials are highly influenced by the nano/microstructures of the membrane material. Proper distribution of these hydrophobic and hydrophilic components constitutes the matrix of the membrane with the functional groups aggregated in small pockets or clusters within the membrane structure. These components govern the different properties of the IEM materials with the hydrophobic component contributing to the morphological stability of the membrane and the hydrophilic domains providing conducting channels.[55, 56] In PEM materials, a high proton conductivity is achieved through different mechanisms involving Grotthuss and vehicular conduction. A more advanced investigation on channel ordering, as well as semicrystalline polymer matrix ordering as a function of membrane stretching, would allow tailoring optimal CEL materials with good transport properties for energy-efficient BPM applications.[57, 58] For instance, developing long-range ionic channel ordering through membrane modification by grafting techniques enhances conductivity.[59] New molecular architectures can be achieved by adjusting size and length of blocks in block-copolymers,[60] the formation of highly

phase-separated nanodomains along with block-induced long-range connectivity of hydrophilic channels,[61] and forming a flexible main-chain structure to improve the cross-organization and to enhance the proton conductivity of the CEL.[62, 63]

CELs for energy devices are typically composed of perfluorosulfonic acid (PFSA)-based materials like Nafion due to their high ionic conductivity and chemical/thermal stability. Nafion is a random copolymer based on an electrically neutral semicrystalline polymer backbone (polytetrafluoroethylene (PTFE)) with randomly tethered side-chain consisting sulfonic (SO_3^-) terminated pendant chains (Figure 4). The unique transport properties of PFSA membranes is due to its phase-separated morphology as a result of the different property of its functional groups and backbone enhanced by solvation. In BPMs, the perfluorinated CELs allow for efficient conduction of protons in addition to its good chemical and mechanical stability. However, these membranes are highly limited by cost and sometimes lack the desired requirement for particular applications. Therefore, the use of fully hydrocarbon-based CELs plays a key role in the effective design and development of low-cost BPM. The typically narrow hydrocarbon based-materials also incurs a good size sieving and hence better selectivity than PSFA-based materials.

A broad variety of hydrocarbon materials are reported in the literature for the design of low-cost CEMs and often with the ambition to reduce the methanol permeability for direct methanol PEM fuel cell applications. Most of these materials involve functional aromatic polymers, among others, based on poly(arylene ether)s,[64-66] poly(ether ether)s,[67-70] poly(phenylene oxide),[71, 72] polyimides,[73-75] poly(phenylene sulfone) [76] and poly(benzimidazole)s.[77-79] In particular, functional materials based on poly(arylene ether) materials have been largely explored due to their relatively straightforward synthesis, good processability, low fuel crossover, high thermal stability, and high mechanical strength, which can also be adapted for BPM design.[80] In BPMs, the choice of

functional group of the CEL can alter the conductivity of the layer and the associated water dissociation kinetics in the IL. The water dissociation activity of functional head groups is related to the rate constant for the rate-limiting step (K_L) of the protonation-deprotonation reactions at the IL. The activity and identity of the functional head group influence the balance between the electric field effect and catalytic mechanisms for water dissociation. In the case where the functional group act as water dissociation catalysts, a trade-off exists between the catalytic film thickness in the space charge region (SCR), the acidity/basicity of the functional groups, the resulting steric effects of the functional groups, swelling properties, and the resulting electric field in the IL.

Sulfonic acid is the most commonly utilized functionality in CEMs due to its strong acidity. Sulfonic acid functionalities can be introduced to the polymer backbone by using either pre-sulfonated monomers [81, 82] or post-sulfonation [83-85] strategies. The use of pre-sulfonated polymers is more advantageous in terms of accurate control of the amount (IEC) and the distribution (random or block) of sulfonic acid groups along the polymer backbone.[81, 86] The post-sulfonation strategy represents a facile and most widely used strategy but it is highly susceptible to undesired side-reactions like degradation or cross-linking [81]. This can be mitigated by the use of an alternative functionalization strategy like metalation (lithiation), which involves the introduction of the sulfonic acid group at electron-poor sites of the aromatic rings, resulting in a stable material with a reduced risk of desulfonation and oxidative degradation.[87, 88]

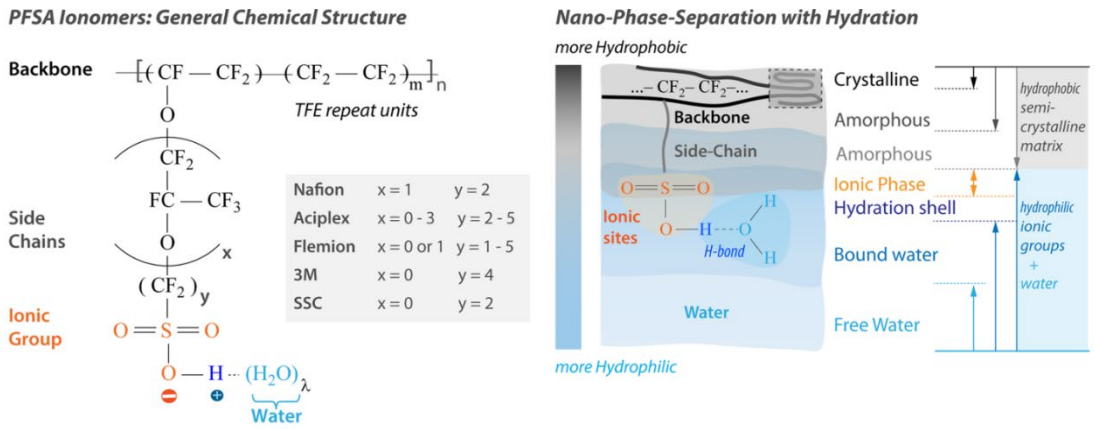

Figure 4. Illustration of the chemical structure of the PFSA ionomers along with the different structural parameters influencing its phase-separated morphology and properties. Reproduced with permission.[26] Copyright 2005, Americal Chemical Society.

The variation in the polymer backbones and topological architecture of ionomers has a considerable impact on the overall performance of CEL, particularly in zero-gap BPM devices. In such configurations, the CEL is in close contact with the catalyst layer of the gas diffusion electrodes (GDEs) on one side and the IL of a BPM on the other side (Figure 5a). Therefore, the chemistry of the CEL backbone, its functionality, and the overall polymer architecture have a considerable impact on the kinetics of the reactions at the different interfaces. A broad range of materials based on block CEMs, main-chain type CEMs,[89-91] side-chain type CEMs,[92-94] comb-shaped CEMs, [94, 95] and densely functionalized CEMs [96, 97] have been reported in the literature. Typical representative materials include hydrocarbon or partially fluorinated materials, as presented in Figure 5b-h. Tuning the properties of these and relevant materials along with precise control of the chemistry of the backbone and nano/micro/macromolecular architecture as well as its impact on the CELs physical and electrochemical properties can address the design requirement of low cost, high performance BPMs for energy applications.

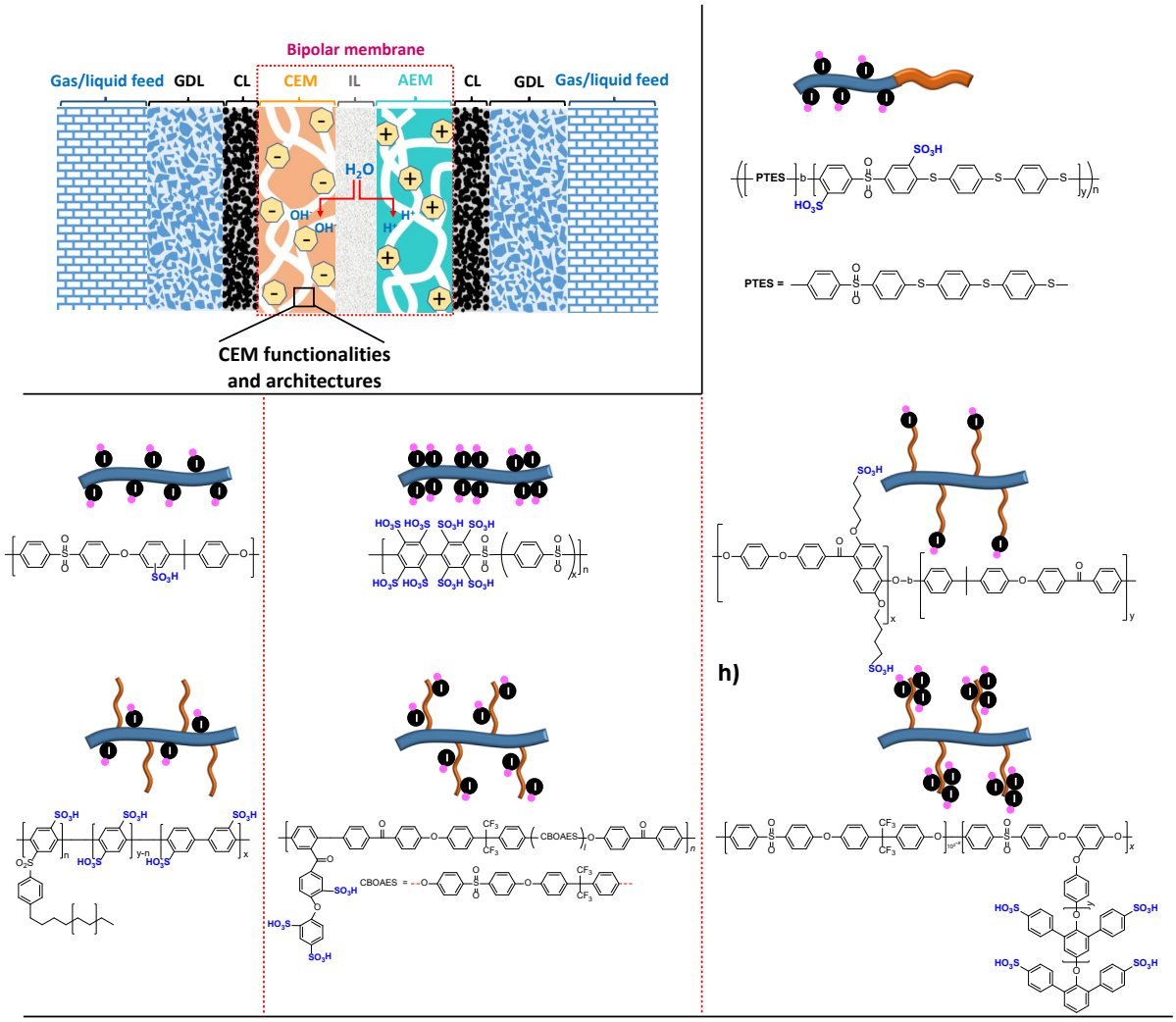

Figure 5. a) BPM electrode assembly in a zero-gap configuration. Generic base materials for the design of low-cost, high-performance cation (proton) exchange membranes for a CEL of a BPM: b) multiblock copolymer based on sulfonated poly(arylene thioether sulfone); c) main-chain type sulfonated polysulfone; d) densely functionalized fully aromatic poly(arylene sulfone); side-chain type e) block sulfonated poly(arylene ether ketone)s containing side-chain groups, f) grafted poly(*p*-phenylene sulfonic acid), g) multi-block copolymers based on poly(tri-sulfonated phenylene)-block-poly(arylene ether sulfone) and h) fully aromatic comb-shaped copolymers based on a poly(arylene ether sulfone) backbone with highly sulfonated poly(phenylene oxide) graft chains.

4.2. Anion exchange layer. An ideal AEMs conducts anions such as OH^-, HCO_3^- and Cl^- while excluding cations. AEMs contain positively charged (cationic) functional head groups covalently bound to a polymer backbone through different orientations similar to the CEMs as shown earlier (Figure 5b-h). Some of the most common base materials utilized as the backbone for AEM are well reviewed in the literature.[29, 98, 99] A range of functional groups (Figure 6a) has been introduced to form AEMs with different physicochemical and electrochemical properties, and more importantly, varying stability in an alkaline environment (Figure 6b).[29, 98, 100] The base polymers can be functionalized to a different degree to form AEMs through different reaction techniques and pathways, for instance, following nucleophilic aromatic substitution reactions in basic medium to prepare condensation polymers.[99]

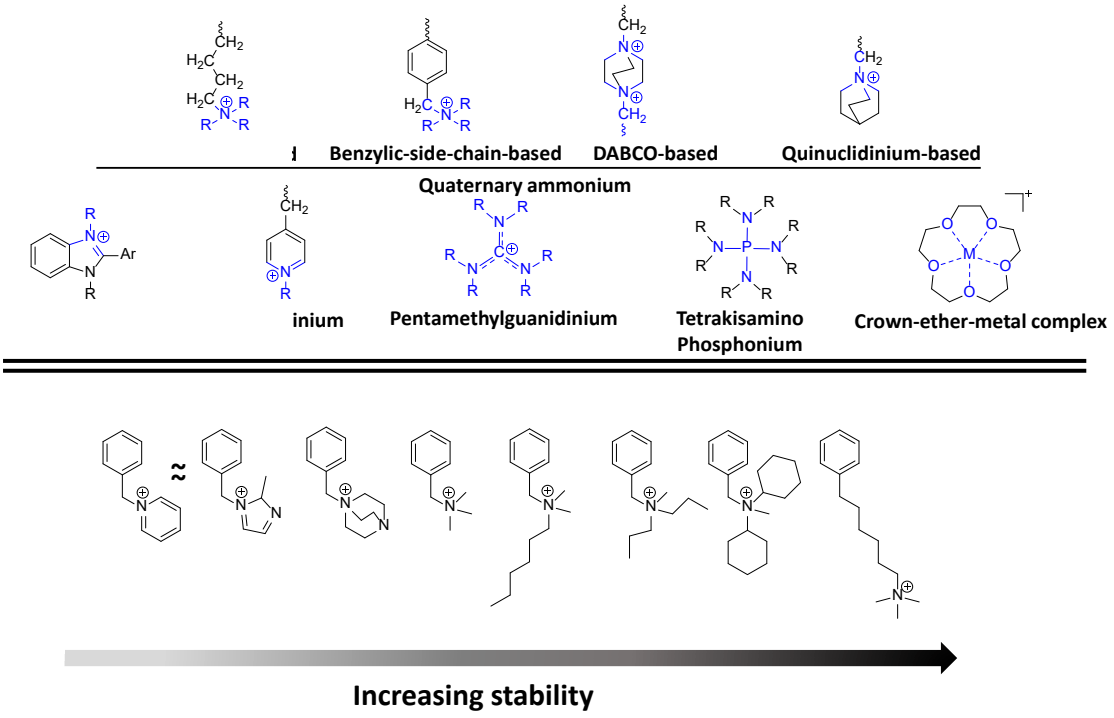

Figure 6. a) Typical functional groups used for the development of AEMs and b) alkaline stabilities of selected compounds with quaternary ammonium functional groups. Reproduced with permission.[99] Copyright 2019, Americal Chemical Society.

In BPM devices, OH^- is transported through AEL to or from the IL depending on system configuration. Different chemical reactions occur at the anode or cathode depending on the composition of the liquid electrolyte and electrodes. For instance, in reverse bias BPM-CO_2 reduction cells, high pH or the use KOH anolyte favors the oxygen evolutions using earth-abundant materials at the anode, coherently with the unique advantage of BPM general functioning as membrane electrolytes keeping a constant pH gradient in the electrochemical cells as mentioned earlier. Thus, the operability of AEL of the BPM in KOH solutions and mediation of OH^- ions transport calls for highly stable as well as conductive AELs to design a high-performance BPM towards practical implementation in electrochemical devices.

The practical application of AEM in electrochemical devices, particularly in strongly alkaline environment, is highly limited by the stability of the common benzyl trimethyl ammonium cations functional groups as well as conductivity due to the lower mobility of hydroxide OH^- ions compared to H^+.[98] Besides, a low degree of the utilization of the ammonium-based functional groups is perceived for ion transport due to its reduced dissociation in the presence of hydroxide ions.[29] The stability issue of the functional groups and backbone are mainly associated with the strong basicity and nucleophilicity of the OH^- ions, which lead to different degradation mechanisms mainly following nucleophilic substitution or Hofmann elimination pathways (Figure 7a), and more recently noted oxidation of the adsorbed phenyl groups at catalyst sites.[101] Various types of functional chemistries have been introduced to address the stability issue. Design strategies mainly involve either the synthesis of new functional groups, steric protection, charge delocalization, control of conformational effects. Recent studies demonstrate that long-chain tetraalkylammonium cations [102-104] and cyclic ammonium [104-106] exhibit better stability compared to quaternary ammonium cations in benzylic positions. Other functional groups such as

phosphonium,[107-109] imidazolium, [110-112] and metal cations [113-115] have also been reported for alkaline AEM fabrication. In particular, the pentasubstituted imidazolium is practically interesting due to its charge delocalization throughout an aromatic ring, which makes it optimal for tuning the properties of CEL in BPM towards high conductivity and alkaline stability.[116, 117 118] This also allows for better control of the amount and depth of functional groups in the catalyst layer of the BPM, governing the electric field enhancement, the ionic conductivity of the IL, and hence the polarization behavior. Various chemistries of the functional groups, for example, the use of multi-substituted imidazolium cations directly into polymer backbones enhances the alkaline stability [119, 120] and DABCO-based functionalities.[121] It should be noted that most of these alkaline stable AEMs exhibit lower hydroxide conductivity than AEMs containing quaternary ammonium cations,[122] mainly due to reduced hydrophilicity as a result of an introduced steric hindrance towards stability.[115, 122] The hydrophilicity of the AEL will have a significant impact on the BPM as it allows for efficient hydration of the BPM IL, which is needed to avoid mass transfer limitations at the IL. One strategy to address these issues is the use of block copolymer analogs to modify the microphase separation of such materials that could also potentially enhance their conductivity. [123, 124] For instance, highly conductive and stable AEMs can be prepared by ring-opening metathesis polymerization of high-ring-strain compounds like *trans*-cyclooctene and its derivative at high polymerization rate and varying block lengths. [122] Engineering side chain configurations based on spacer units between the functional groups and the polymer backbone as well as the extender chains pendant to functional groups would also allow tuning AEM towards designed criteria. The use of long flexible side chains terminated by QA groups on poly(phenylene oxide) (PPO) backbones displayed good microphase-separated morphology. [125] High molecular weight arylene ether-free aromatic AEMs based on poly(biphenyl alkylene)s have also shown

good chemical and mechanical stabilities (Figure 7b). [126] Chemical structure (proper arrangement) of backbone is beneficial for fabrication of highly conductive AEMs with ion-conductive polyelectrolyte membrane morphology. The difference in backbone orientations of terphenyl-based polymers with pendant QA alkyl groups has been shown to significantly influence the ionic conductivity, laying out a new design concept.[127] Such membranes fabricated based on meta-terphenyl aromatic monomer were claimed to be the best materials fulfilling most of the required design criteria, particularly, for alkaline fuel cell applications, presenting one strategic alternative for the design of high performance alkaline BPMs. Other classes of materials like KOH-doped PBI have also been utilized to replace alkaline AEMs.[128-130]

A straightforward way to enhance ionic conductivity of AEMs is by increasing the IEC. This may, however, lead to excessive swelling that limits the mechanical stability of such membranes. It is worth noting that the strength and amount of the functional groups of the AEL of the BPM influence the electric field enhancement, the ionic conductivity, the water dissociation kinetics at the BPM IL, which will be elaborated in section 5. Emerging polymers for such applications would involve ionenes that present a good prospect for designing materials with combined ionic conductivity and stability, even at higher temperatures.[131] For instance, tuning the chemistry of polybenzimidazoles at low pH or introducing a complete *N*-alkylation with controlled swelling allows for the fabrication of cationic ionenes with a diverse physicochemical property (Figure 7c). More recently, spirocyclic ionenes synthesized by cyclo-polycondensations (Figure 7d) were reported to have exceptionally high stability and conductivity in alkaline media.[132] As expected, such materials were prone to dissolution in water due to its high IEC. To break this barrier, chemically/ionically cross-linked blends of such polymeric ionenes/polybenzimidazole (PBI) can be used for designing an AELs for high performance BPM. The as-such formed ionenes are

emerging as a new class of AEM materials that can be suitably adapted to design BPMs for practical energy devices. Overall, there is an enormous amount of materials systematically investigated for alkaline stable and highly conductive AEMs [98, 133, 134] which can be well adapted for designing high performance BPMs.

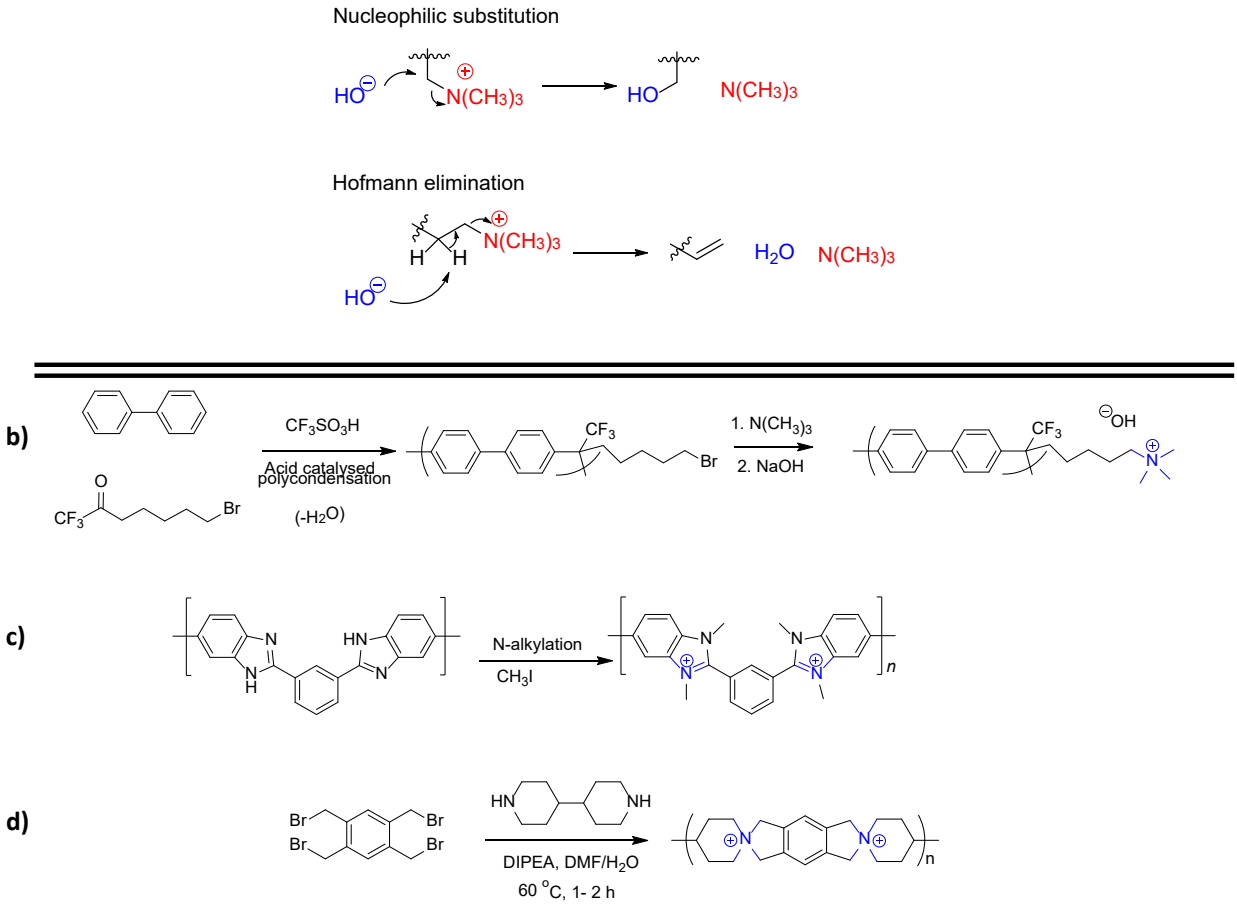

Figure 7. a) Degradation mechanisms for AEMs in an alkaline environment: the nucleophilic OH^- ions react through different routes depending on the chemistry of polymer backbone and functional groups. b) Synthetic route for aromatic polymer AEMs through acid-catalyzed polycondensation and Menshutkin quaternization; c) Polybenzimidazoliums obtained by *N*-alkylation of polybenzimidazoles; d) Synthesis of spirocyclic ionenes by cyclo-polycondensation.

5. BPM Interfacial structure and morphologies

The interface between membrane layers in a BPM is the most critical component for the optimal design of high performance BPM. The interface structure, composition and morphology determine the kinetics of water dissociation and ionic separation under reverse bias operation. The general structure-morphology-property relationships and the rate/activity of water dissociation at the interface is well presented by Giesbrecht *et al*. *et al*.[7]

IL can be designed in different structures depending on the type and structure of the interface catalysts as well as the membrane layers itself and how it is contacted with each other. The nature and type of these contacts could vary depending on the type and morphology of the membrane layers. In an abrupt junction model (Figure 8a), the thickness (δ) of the IL is assumed to infinitesimal. [135] The drawback of an abrupt junction model is that it doesn't consider the presence of water or a catalyst layer and also excludes the heterogeneities and morphologies of both the BPM interface and outer layers including the strength of the functional groups and structure of ionic channels in the IL and ionomers.[7, 31, 135] A smooth model is a deviation from an abrupt model (Figure 8b). Such models can be represented in 1D or 2D morphology formed between homogenous/heterogeneous membranes.[135] Smooth interfaces can be formed by simple lamination of CEL and AEL layers with smooth surfaces. Smooth BPM junction is mostly associated with morphological heterogeneities and poor contact due to differences in physicochemical properties of the membrane layers. In some cases, the surfaces of the outer layers of BPM can be roughened or micropatterned[136] so that the other layer can blend in. A more efficient contact at the interface can be achieved using other techniques for BPM formation such as solution casting or by the use of bulk heterojunction structure formed by electrospinning, creating a high surface area of the ionomer layers in the IL. [32, 137, 138] These also ensure enhanced catalytic water dissociation beyond

creating good contact at the IL, providing efficient transport of water and ions to and from the BPM interface for possible and stable operation at high current densities. However, the difference in outer layer properties such as the swelling ratios and mechanical properties could put stress on the IL leading to the delamination of BPM during operations.[7] A proper balance in physicochemical and electrochemical properties of both the BPM outer layers at a controlled interface-identity and composition is essential to ensure good contact at the IL in BPMs. A profiled interface is formed when the surface roughness of one of the layers fills up the corrugates of the other membranes.[139] This kind of interface can be formed by casting one membrane over a pre-formed, rough membrane. Casting a second layer from a solution instead of a pre-formed film results in stronger contact and hence a stable bipolar membrane, in particular, if reinforcement is introduced in the initial layer. A certain roughness increases the contact area at the interface. Thus, profiled interfaces might result in a continuous and increased contact area that could lower the overpotential needed to drive the water dissociation and ionic separation. Arges *et al*. [136]recently reported BPMs with profiled (micropatterned) interfaces prepared by forming patterns in the form of circular wells on the CEL of the BPMs. Such a strategy was shown to enhance the interfacial contact area by about twice that of the corresponding BPM interfaces without the micropatterns, corresponding to about 250 mV reduction of the onset potential.[136] Membranes with heterogeneous interfaces generally exhibit a higher membrane potential compared to membranes with homogenous interfaces due to the partially non-conductive membrane surface in heterogeneous interfaces.[140, 141] The BPM interface can be filled with a separate catalyst layer in 2D (Figure 8c), or 3D structures composed of bipolar or monopolar (Figure 8d) ionomers imposing different water dissociation kinetics. BPMs with homogenous interfaces are more relevant for energy devices due to low interface losses requiring further optimization in terms of morphology and activity.

Homogenous interfaces are more relevant for applications in electrochemical energy systems. The use of a bulk heterojunction, as reported in some of the recent works utilizing electrospun fibers,[83, 142, 143] demonstrates a possibility of designing stable, high surface area interface BPMs operable at high current densities.

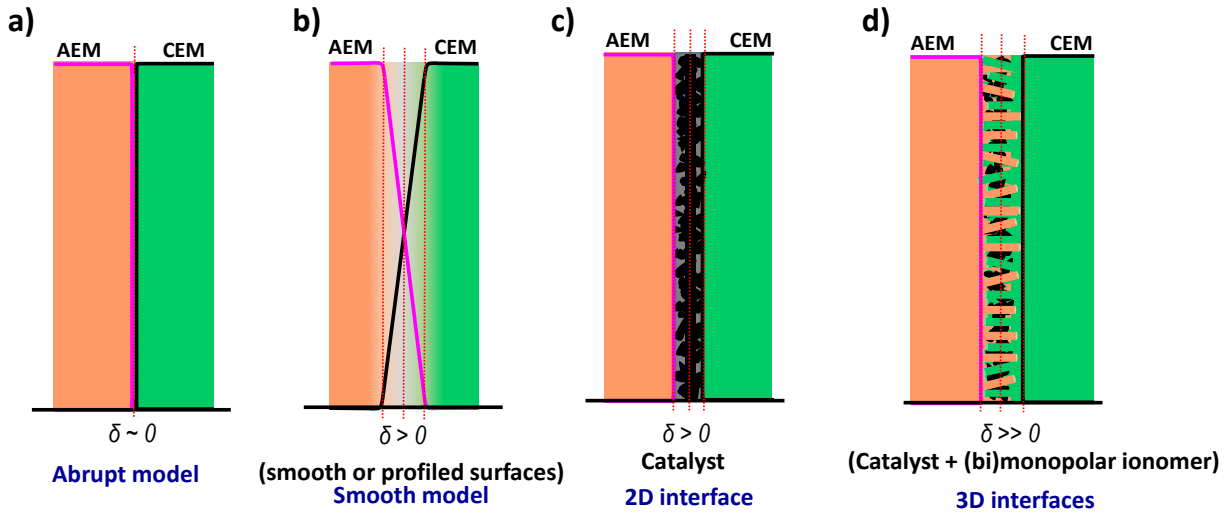

Figure 8. Formation of different interface structures in BPM contact region: a) abrupt model; b) smooth models: smooth or profiled surfaces with (partially) heterogeneous structures; c) catalytic interface with catalyst 2D structures and d) 3D structure with (mono)bipolar ionomer; a rough visualization of the interface thickness (δ) is given depending on the type of interface.

Figure 9a presents an interplay of different parameters governing the rate of water dissociation catalysis at the BPM interface. This depends on an interplay of several factors at the BPM interface and properties of IELs governing the water dissociation kinetics in general. The thickness and electrical conductivity of the catalyst layer, CSD in IL, swelling properties, and functional group strength highly influence the EFE water dissociation at IL.[7, 135] This is also relevant to the depletion thickness formed during BPM operations. It is important to note that the counterbalanced role of the EFE and catalytic water dissociation effects leads to a different

depletion layer thickness for BPMs with and without a catalyst.[143] Under reverse bias, for a BPM with an interface catalyst, a larger portion of the functional group is counterbalanced by H^+/OH^- ions due to enhanced H^+/OH^- flux, resulting in a low electric field and thin depletion layer at the interface compared to the BPM without a catalyst. This phenomenon remains similar for BPMs with 3D interfaces (Figure 9b) mostly prepared by electrospinning technique (Figure 9c), however, the electric field is further influenced depending on the structural interaction of the fibers with the

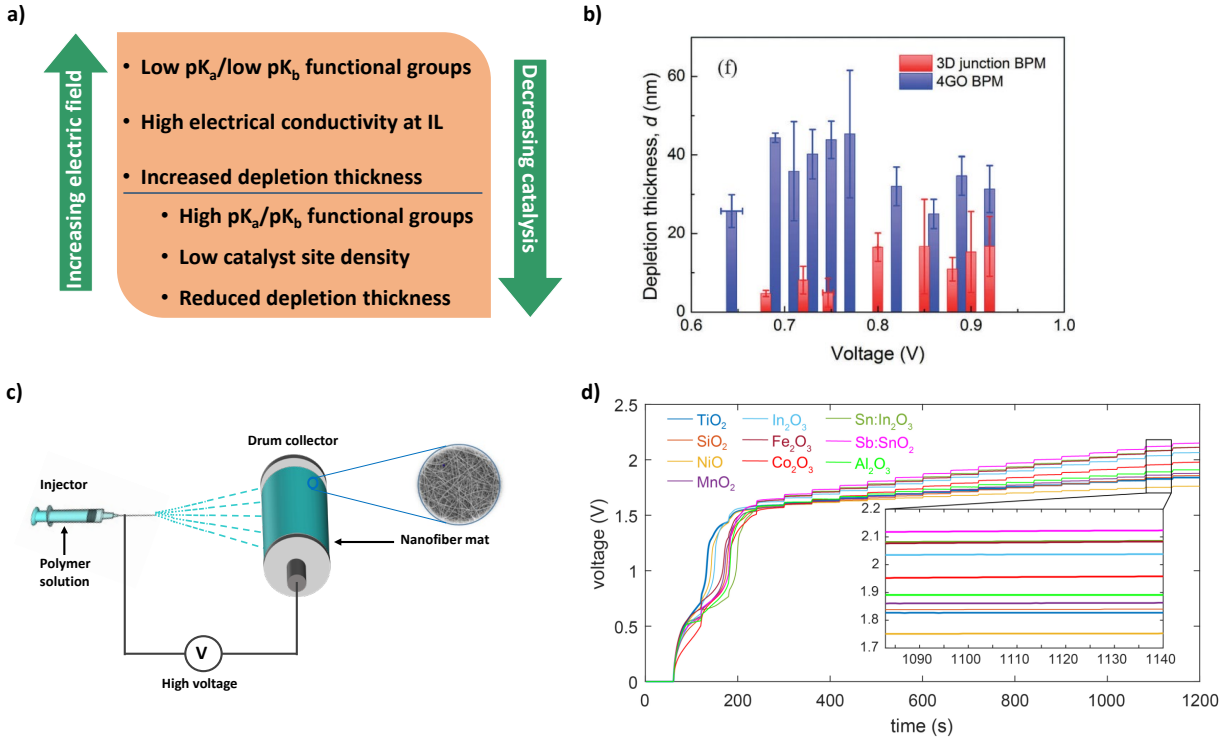

membrane surface. A more advanced membrane synthesis protocol is required for tailoring the morphology of electrospun 3D interfaces to control the alignment and positioning of the fibers with respect to the membrane surface, for a balanced electric field enhanced and catalytic water dissociation reactions.

Figure 9. a) The variations in an electric field and the rate of water dissociation catalysis at the BPM interface: governing parameters and the trade-off; b) The variations in depletion region thickness as a function of the reverse bias voltage; Reproduced with permission.[143] Copyright

2017, Royal Society of Chemistry. c) Electrospinning as a technique for tuning the structure and morphology of the BPM interface; d) BPM electrolyzer stability testing with various water dissociation catalysts: a chemically stable water dissociation catalyst Sb: SnO_2 is used at one surface at the CEL, while the water dissociation catalyst at the AEM is varied. Reproduced with permission. [5] Copyright 2020, The American Association for the Advancement of Science.

The other factor affecting the electric field at the BPM interface is the catalyst composition. High content of electrically conductive material in the IL reduces the electrostatic potential difference across the catalyst layer thereby increasing the EFE close to the outer layers, whereas the high content of electrically insulating material in the catalyst layer reduces the electric field strength in the IL.[143] However, care should be taken when introducing supporting materials as it could also influence the membrane properties such as permselectivity and ionic conductivity. In this regard, the enhanced ionic conductivity of the catalyst film reduces the electrostatic potential drop associated with ion transport in the IL. Therefore, the design and development of a water dissociation catalyst layer with high electric and ionic conductivity are required for the reduction of the voltage losses across the catalyst layer irrespective of the IL thickness. Overall, a more precise investigation supported by experiment and modeling is required to clarify the interdependence of the EFE and catalytic water dissociation mechanisms as well as the physicochemical parameters of the BPM materials. An accurate model is perceived to consider, among others, the homogeneity of the water solution and electric field across the IL and the SCR, junction morphology, rate constants for forward and backward reaction, physicochemical and electrochemical properties of the membrane layers.

5.1. Catalyst choice and activity. As discussed earlier, the water dissociation rate (at a given potential) occurring at the interface of a BPM can be enhanced by introducing a catalytic layer at

the BPM junction. Some of the most commonly used catalysts include inorganic materials (like metal hydroxides [83, 144] or graphene oxides,[137, 145] heavy metal ion complexes like those of iron, chromium, zirconium[146, 147]). In particular, GO-based materials have acquired a huge interest due to its high CSD, where the carboxylate groups exhibited the highest reactivity towards the water dissociation. [148-150] Water dissociation on the metal oxides and hydroxides is activated by the adsorption of water onto the surface followed by proton transfer from the water to the adjacent oxygen atom resulting in hydroxide ions. A clear elucidation of the metal oxide surface species and utilization efficiency of metal oxide material helps to identify catalytically active species during water dissociation and the associated electric field impact in the BPM IL. The surface chemistry of metal oxides is highly dependent on external pH as its surface is generally a polyacid and/or polybases, which could also influence the water dissociation kinetics. In BPM, the catalyst layer is in contact with CEL (acidic) and AEL (alkaline) that could therefore alter the activity of the metal oxide catalysts. A systematic study using chemically stable water dissociation catalyst layers of a BPM while varying the catalysts on the other layer, and comparison to the point of zero charges (PZC) of each catalyst, indicates that the best water dissociation catalysts on the acidic CEL are those with acidic PZCs and vice versa (Figure 9d).[5] This is consistent with the fact that metal oxides tend to work best for water dissociation when the local pH is near the PZC, other factors also come into play such as the variations in pK_a of exposed surface, the activity of surface oxygen species, are also likely to affect water dissociation activity. Therefore, extensive computational and experimental studies are required to unravel the mechanisms insights behind the enhanced water dissociation as well as catalyst utilization at the BPM IL.

Organic hydrogen-bonding materials based on weak acids (HA), or weak bases (B) such as phosphoric acid [151] or pyridines, [152] etc can also be utilized as an interface catalyst. These catalysts

can be incorporated either in ion-permeable membrane layers [153] or in between the two ion-permeable layers. [154] Depending on the strength of acidity/basicity, the functional group of the membrane layer itself might also provide a catalytic activity.[30]

The catalysts can be immobilized at the interface by using different techniques including spray or electrodeposition, [155] dip-coating, [155, 156] casting to form a uniform distribution of the catalyst throughout the membrane layer, [30] electrospray deposition, [157] etc.

Tuning the water dissociation chemical properties and morphological features of the catalyst layer in the BPM IL is the key to reducing the voltage losses associated with BPM operation. Coupled internal electric fields enhanced and catalytic water dissociation pathways can be achieved through the design of a catalyst layer with high site density at a film thickness near the SCR width. The use of composite water dissociation catalysts could improve film adhesion ensuring device longevity. Tailoring the electrical and ionic conductivity, as well as the identity of the water dissociation catalyst near the CEL and the AEL will improve water dissociation efficiency thereby reducing the voltage losses across the interface.

A possible issue with an interface catalyst can be degradation at the interface with a long time of operation. A relatively constant degradation rate (~ 2-5 mV/min) was reported from a series of MO catalysts investigated in BPM electrolyzers operated over 20 min (Figure 9d).[5] However, there was no clear identification of this degradation was due to the catalyst dissolution or chemical transformation. A more detailed investigation is required to understand the possible catalyst degradation routes and mechanisms at the BPM IL, over a broad range of time operational time.

5.2. Interfacial modeling of BPMs. Most of the research on modeling research on the BPM was focused on catalytic as well as electric field effects at the BPM interfaces, correlation and

impact on the water dissociation activity.[6, 31] Based on models employing Nernst-Planck equations and the Donnan equilibrium at BPM interface, it was shown that the water dissociation at the BPM interfaces occurs in a depletion layer in the presence of a strong electric field assumed to be proportional to the applied voltage, depicting that influential effect of both the catalytic and the second Wien effects.[33] This has been counteractive to other studies that depicted the water splitting to be governed by the overpotential at the BPM interfacial layer.[158] A number of other studies on modeling of the interfacial layer have also been reported focusing on the local chemical equilibrium of water dissociation considering adjacent solution diffusion layers[159], quantum chemistry simulations to describe the effects of electric field strength on water dissociation[160], combined Nernst-Planck-Poisson equations and local water-splitting kinetics to estimate the depletion layer thickness[143], and elucidating the transient effects due to the incomplete depletion of mobile ions at the BPM interface[161]. Recently, Nikonenko *et al*. developed a comprehensive type model by combining the Nernst-Planck-Poisson equations are coupled with the relevant equations describing the local water splitting kinetics at the BPM interface. The inclusive model considers the catalytic effects of the functional group and the interface catalysts along with the protonation-deprotonation reactions, and the electric field (second Wien) effect on the water dissociation at the BPM interface. The model results depict an observable current density of up to 100 mA cm^{-2} at 1 V with a very thin (2 nm) catalytic layer regardless of the functional effect of AELs and CELs.[31] Despite the vast majority of reverse bias experimental investigations and characterization on BPM, and modeling studies, the phenomenon governing the water dissociation at the BPMs is still poorly understood. More recently, Bui *et al*. implemented a model elucidating the multi-ion transport across a BPM in relation to the interface properties for the design of energy-efficient, high performance BPMs.[27] The model result, as shown in the polarization curves of the

BPMs (Figure 10b), depicts a higher utilization efficiency of a catalyst in thinner interface design, which allows for a more centralized catalyst alignment in SCR resulting in a high electric field.

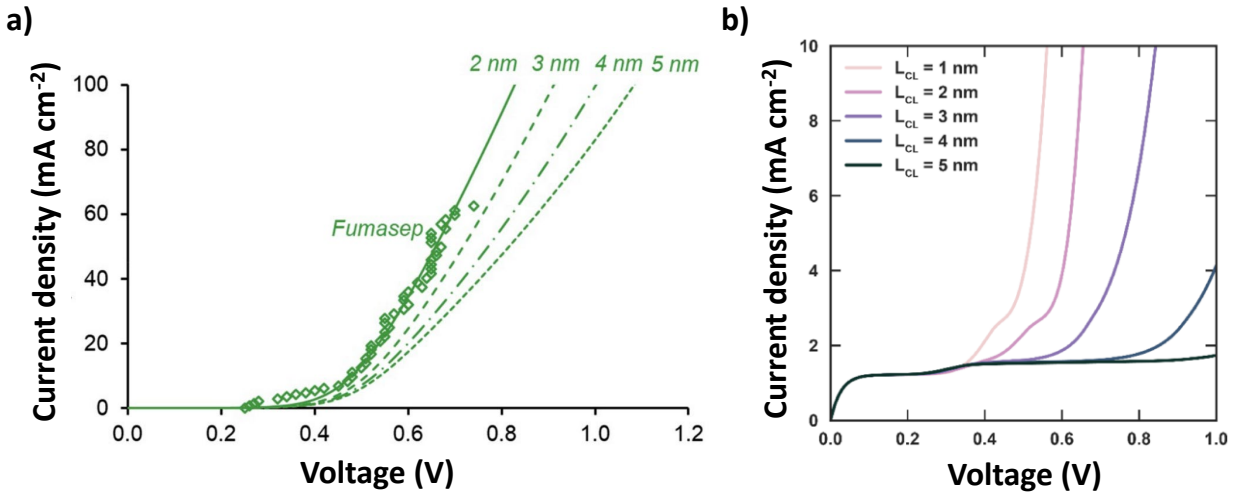

Such interface design combined with the use of an effective catalyst will not only reduce the onset potential of the BPM but also increase the current efficiency in perceived electrochemical applications. Overall, the different findings from such a modeling studies lays a ground for future research directions towards the desing of optimial BPMs for an intended energy technologies.

Figure 10. a) Polarization curves of a Fumasep membrane with a varying thickness (2-5 nm) of the catalyst-filled neutral region. Reproduced with permission.[31] Copyright 2020 Elsevier. b) polarization curves obtained by modeling of a BPM with a varying thickness of interface catalyst at pH 7-7 (catholyte-anolyte); Reproduced with permission.[27] Copyright 2020, American Chemical Society.

6. Assessment of methods for BPM and interface preparation

The preparation of BPMs follows a stepwise procedure involving the formation of each component. As a first step, the synthesis of the individual CEM and AEM layers involves a suitable selection of base materials, followed by functionalization, (e.g. grafting) polymerization/polycondensation, blending and/or crosslinking, depending on the design

requirements and applications. A separate IL with a varying composition may or may not be introduced between the IELs, but the IL is used in most cases to facilitate water dissociation as discussed earlier. Details on membrane layers and different IL used in the literature are summarized in Table S1 (supporting information). Although most BPMs are prepared from commercial base materials either for CEL or AEL, or both, full tailoring of the whole components has also been reported based on, for example, hydrocarbon materials such as SPEEK, PPO, PVA, etc.[142] When preparing layers, casting is the most common technique employed along with (hot)pressing to form the final BPM. Interface catalysts can be introduced onto a preformed membrane by different techniques such as airbrushing or spin coating, and more recently, electrospinning. The I-V behavior of the BPM is the most widely studied during BPM characterization as it reflects the performance of BPM in terms of water dissociation efficiency, among others. Despite the availability of a large variety of BPMs developed from both PSFA and hydrocarbon-based materials, there is still a lack of highly efficient BPM fulfilling the majority of the desired properties for advanced electrochemical energy systems like CO_2 electro-reduction.

BPM can generally be formed as a single layer (film) BPM [162-164] or multilayer materials. [137, 138, 144, 139, 145] Single-layer BPM is prepared by a subsequent introduction of anionic and cationic functionalities to each side of the pre-selected base material. However, most of the existing BPMs are multilayered structures that are prepared from commercial or tailor-made IEMs. In either case, good contact between the IELs and the IL should be established to produce high-quality BPMs that can support high currents without delaminating. Despite the promising applications demonstrated in various emerging electrochemical energy systems, most of the BPMs are limited by high electrical resistance and hence the current efficiency. One alternative to address the high

electrical resistance associated with multilayer BPM is the development of methods for accurate design of BPM based on a single ionomer layer with two different functionalities.

Lamination is a simple method to prepare BPMs, for example, by first treating the CEL and AEL with heavy metal (e.g. Ni^{+}, Sn^{2+}, Cr^{3+}) solutions which may be present in the form of nitrate or chlorides or acid/base solutions, and then conjoining by applying heat below the glass transition temperature of the membranes or by simple manual lamination.[138, 153, 165] In the hot-pressing method, separate AEMs and CEMs are bonded together by applying pressure and heat under a hydraulic press.[83, 166] It can also be used in combination with other techniques such as solution casting [167] and electrospinning.[166] However, both the lamination and hot-pressing methods may not guarantee an effective contact between the membrane layers as bubble or blister might form during fusion, which reduces the membrane lifetime and current efficiency. Moreover, dislocation of functional group may also result during pressing which could lead to high electrical resistance. Solution/tape casting or slot die coating are the most widely used method for the fabrication of IEM for various applications including electrochemical energy systems. While the former technique is suitable for small-scale batch-type processes, the latter are widely used in industries, owing to screening large dispersion batches for quality and performance, high production rates in continuous processes and potentially good control of the physicochemical properties of the resulting membranes. As shown in Table S1, most of the outer layers of the BPM (AEMs and CEMs) are prepared by solution casting.[137, 144, 168] Unlike simple lamination and hot-pressing, BPM preparation by casting the ionomer layer or the interfacial polymer layer is expected to ensure good adhesion between the BPM components.

6.1. Techniques for designing of BPM interface. The IL of a BPM can be formed in different morphology by using different coating techniques like manual airbrushing, spin coating,

electrospraying, atomic layer deposition, and electrospinning.[83, 137, 169] More recently, electrospinning is gaining more attention as a simple, fast, and low-cost method to produce nano/microfibers porous mats with a high surface to volume ratio. As shown in Figure 9d, this technique involves discharging a polymer melt or solution through a metal needle spinneret that is subjected to a strong electric field or voltage (in kV range) leading to the formation of thin fibers collected on drum collector as fiber mat. The nanofibers can also be made from various organic and inorganic composite materials applicable to energy devices.[170, 171] When it comes to BPMs, electrospinning can be used to prepare the IELs [166, 169] but most importantly, a 3D IL with a high surface area from interpenetrating anion and cation exchange polymer fibers.[83, 144] The high surface area formed as such, along with proper water transport properties of the membranes, mitigates the depletion of water at the interface, which is crucial for mechanical stability as well as high-CD operations. For instance, a BPM was prepared by electrospinning of SPEEK fiber mat as a CEL followed by a dual fiber mixture of SPEEK/QPPO co-electrospun from two separate spinnerets as a 3D interface, simultaneously air-spraying a 10 wt% $Al(OH)_3$ aqueous nanoparticle suspensions. Thus, a very thin IL was formed in this way, on top of which QPPO fiber mat was electrospun as an AEL. These BPMs feature a combination of a thin interfacial layer with about 10 μm thickness of interpenetrating polymers, along with dense outer layers of membranes with about 17 μm thickness. A very promising performance of the BPM was reported in terms of reduced co-ion leakage (high selectivity) and stable operations under a very high CD of up to 1.1 A cm^{-2}. It is important to note that a wide range of soluble polymer with a sufficient molecular weight can be electrospun, and by tuning the operational parameters like the polymer molecular weight, composition/viscosity of ink, applied voltage, follow rates, etc, this technique allows for the design of a high-quality BPMs with fibrous interfaces formed from different polymer compositions and

blends. Besides electrospinning, soft lithographic approaches to create micropatterned interfaces for BPM[136] could also be a promising technique, however, limited by capital and operational cost as well as complicated requirements for some systems e.g. formation of structures at nanometer sizes. Despite the high surface area of the dual-fiber electrospun IL, poor contact between the membrane layers and hence the delamination of the BPM is a key challenge. This points at the importance of a careful selection of base materials with sufficient adhesion and miscibility of the ionomer-catalyst layers.

7. BPMs with single and miscible layers

One limitation of bi/trilayer BPMs is the membrane degradation and delamination due to insufficient transport of water and the poor adhesion at BPM interface, during long-term operations at high CD under reverse bias. Bi/trilayer BPMs are also limited by high electrical resistance leading to high voltage loss compared to monopolar membranes. One strategy to address the delamination issue is the use of a BPM with miscible backbones (compatible/same backbone material) to ensure good adhesion at the interface. The use of single-layer BPMs can also be a good alternative not only to ensure a good interface structure but also to reduce electrical resistance.[162, 172, 173] Attempts have been performed to prepare single sheet BPM by introducing different charge layers on a single film of polyethylene,[173] ETFE [174] or polyvinylidene fluoride [162] using different techniques like radiation grafting or plasma-induced grafting polymerization. In this regard, there an opportunity to explore a broad range of polymeric substrates that can be functionalized on each side like PPO and PSEBS. The limitation to the design of single-layer BPM is the introduction of water dissociation catalyst at a controlled depth and morphology. A possible way to introduce the catalysts is either by dissolution into the polymer film in contact with catalytic solutions or using substrates based on composite film incorporating catalytic materials.

8. Asymmetric BPMs

Asymmetric BPM designs involve the formation of outer layers in different thicknesses.[36] One advantage of altering the thickness is the control of selectivity, as described earlier. For instance, in electrodialysis, it has been shown selectivity limitation can be mitigated by the use of asymmetric membranes,[36] enabling the production of high purity acidic or basic products. More recently, the application of such asymmetric BPM has been extended to water electrolyzers following the typical preparation procedure of introducing CEL as ionomer in combination with a bulk AEM, or vice versa. Such a BPM water electrolyzer design displayed a very higher current density of up to 9000 mA cm^{-2} at cell voltages of 2.2 V presenting a huge commercial prospect.[8] Asymmetric BPMs designs, however, impose a stability issue in terms of BPM delamination due to the difference in the outer layer properties and thus require careful tuning of physio-chemical compositions and electrochemical properties for maximum gain.

9. Conclusion and outlook

In this work, a thorough evaluation of the key design requirements for high-performance BPM is performed along with the membrane structure-property-performance analysis with a particular focus on interface design and the associated water dissociation kinetics at the BPM interface. The unique aspect is that the water dissociation at the BPM interface allows for maintaining a pH gradient which allows for distinct optimization of the reaction environments and catalysts used for coupled reduction and oxidation reactions.

Control of the local acidity/basicity of the BPM outer layer and the BPM-electrode interface properties allows for optimization of the local electrode reaction towards reduced electrode overpotentials, which is especially important in zero-gap BPM devices. The chemistry of the IEM backbone, nature, and activity of the functional group, and the overall polymer architecture have

a considerable impact on the kinetics of the reactions at different BPM interfaces. Tuning the hydrophilicity of the monopolar IEMs enhances the swelling properties of the BPM, which reduces the water depletion zone, keeps sufficient hydration at the interface, and increases the maximum operating CD. Enhanced selectivity or reduced co-ion leakage in BPM layers can be acquired mainly by fine-tuning the membrane microstructure in terms of optimum diameter of ionic channels and pore sizes, controlled swelling properties, the amount and identity of functional group. A wide range of design strategies are reported for monopolar membranes but the adoption of BPMs depends on the cost and feasibility for large-scale implementation which requires a specified techno-economic assessment. For instance, conductive CEMs can be obtained by incorporating a long-range ionic channel ordering through membrane modification by different techniques like radiation grafting with a higher potential for mass production of such materials. For reduced membrane cost, the choice of fully hydrocarbon base materials is critical. For AEMs, the structure and morphology of the backbone and respective functional group not only determine the conductivity but also stability in aggressive alkaline environments. Physical properties of the outer layers also play a role, for example, reduced thickness layers reduce the ohmic losses at large current densities but this is associated with the increased co-ion leakage. The most efficient BPM is believed to be the one of asymmetric type with a CEL less thick than the AEL for a balanced co-ion leakage, membrane conductivity, and good mechanical property.

When it comes to the design of highly effective BPMs with excellent water dissociation efficiency, the structure and morphology of the interface are critical. The quality of the interface is dependent on chemistry at the interface coupled to the thickness and effectiveness of the catalyst layer, catalytic active site density, the nature of the outer layer functional group in contact with the catalyst layer, end the electrical properties of the catalyst layer in general. Thus, systematic control

of all these properties allows for designing a near-ideal BPM with significantly high water dissociation efficiency and stability. The very promising strategy in this regard is the implementation of 3D interfaces in the form of bulk heterojunction formed by different techniques with the most prominent being the ones based on electrospun nanofibers, which exhibit excellent contact and activity mainly due to increased catalytic active sites in such structures. Introducing a certain roughness when forming IELs combined with corrugated interfaces could also promote good contact at the BPM interfaces. Other strategies involve the design of BPM with miscible backbones. Good contacts not only stabilizes the membrane but also reduce interface resistance.

Elucidating the interdependence of the water dissociation activity of the functional group of IEMs, electrical properties and the catalytic activity of the IL is essential for designing novel BPMs. A strong electric field increases the water dissociation at the BPM interface, which is limited by the thickness, electrical conductivity, swelling properties and catalytic site density at the IL. Thus, a unique interface design based on thinner catalytic layers with increased electrical conductivity and active site density allows fabricating an energy-efficient BPM. There is a trade-off between the EFE and catalytic water dissociation effects leading to different depletion layer thickness in BPMs depending on the structure and catalytic composition of the IL. For instance, the electric field in 3D interfaces is highly influenced by the structural interaction of the fibers with the membrane surface calling for more advanced design routes for tailoring the morphology of such interfaces.

The application of BPMs is diversely expanding, beyond the classical acid-base production using electrodialysis, in recent days in many key areas such as water electrolyzers, fuel cells, and batteries. In monopolar membrane-based CO_2 electrolyzers, the main challenge is the parasitic CO_2 crossover in addition to product crossover which varies depending on the operating current

density, among others. These issues can be effectively avoided by using BPM-based CO_2 electrolyzers, in which the current is partly contributed by water dissociation resulting in the outward flux of ions from the BPM interface. The use of BPMs in a fuel cell, as configured in forward bias mode, enables effective water management with water formation at the BPM interface that minimizes ohmic losses. Such a fuel cell design also allows for separate electrode compartments allowing for optimal catalysts choice and electrode kinetics. However, the formation of water at the BPM interface also makes the system prone to stable operation due to BPM delamination calling for design optimization of BPM e.g. using asymmetric structures. BPM equipped (reverse bias) acid-base flow battery system recently emergy as a viable route for energy storage. As co-ion leakage is the main issue in such a system particularly pronounced under high electrolyte concentrations, a design route for highly selective and conductive BPMs is essential. The ground to the energy application of BPMs has also linked the potential utilization of the BPM itself for extracting the raw materials (e.g. CO_2 and NH_3) for such energy technologies. In this regard, bipolar membrane electrodialysis processes for recovery of resources like NH_3 and capture CO_2 capture present a promising strategy. However, the crossover of neutral species driven by diffusive flux, among others, is the main challenge that can potentially be mitigated using BPMs with optimal thickness as well as crosslinking degree.

ASSOCIATED CONTENT

The following file is available free of charge.

Typical I-V curves and selected literature on materials and interfaces for bipolar membranes (PDF)

AUTHOR INFORMATION

Corresponding authors

*E-mail: rastu@dtu.dk; rashtey@gmail.com (Ramato Ashu Tufa)

D.A.Vermaas@tudelft.nl (David Vermaas)

larda@dtu.dk (David Aili)

Notes

The authors declare no competing financial interest.

ACKNOWLEDGMENTS

This work was financially supported by the European Union's Horizon 2020 research and innovation program under the Marie Sklodowska-Curie (713683, COFUND fellows DTU), Independent Research Fund Denmark (0217-00074B) and the Netherlands Organization for Scientific Research (NWO) under project number 733.000.008 in the framework of the Solar to Products programme co-funded by Shell Global Solutions International B.V.

REFERENCES

1. Chu, S.; Majumdar, A., Opportunities and challenges for a sustainable energy future. *Nature* **2012,** *488* (7411), 294-303.
2. Durst, J.; Siebel, A.; Simon, C.; Hasché, F.; Herranz, J.; Gasteiger, H. A., New insights into the electrochemical hydrogen oxidation and evolution reaction mechanism. *Energy & Environmental Science* **2014,** *7* (7), 2255-2260.
3. McCrory, C. C. L.; Jung, S.; Ferrer, I. M.; Chatman, S. M.; Peters, J. C.; Jaramillo, T. F., Benchmarking Hydrogen Evolving Reaction and Oxygen Evolving Reaction Electrocatalysts for Solar Water Splitting Devices. *Journal of the American Chemical Society* **2015,** *137* (13), 4347-4357.
4. Blommaert, M. A.; Aili, D.; Tufa, R. A.; Li, Q.; Smith, W. A.; Vermaas, D. A., Insights and Challenges for Applying Bipolar Membranes in Advanced Electrochemical Energy Systems. *ACS Energy Letters* **2021**, 2539-2548.
5. Oener, S. Z.; Foster, M. J.; Boettcher, S. W. J. S., Accelerating water dissociation in bipolar membranes and for electrocatalysis. **2020,** *369* (6507), 1099-1103.
6. Pärnamäe, R.; Mareev, S.; Nikonenko, V.; Melnikov, S.; Sheldeshov, N.; Zabolotskii, V.; Hamelers, H. V. M.; Tedesco, M., Bipolar membranes: A review on principles, latest developments, and applications. *Journal of Membrane Science* **2021,** *617*, 118538.
7. Giesbrecht, P. K.; Freund, M. S., Recent Advances in Bipolar Membrane Design and Applications. *Chemistry of Materials* **2020,** *32* (19), 8060-8090.

8. Mayerhöfer, B.; McLaughlin, D.; Böhm, T.; Hegelheimer, M.; Seeberger, D.; Thiele, S., Bipolar Membrane Electrode Assemblies for Water Electrolysis. *ACS Applied Energy Materials* **2020,** *3* (10), 9635-9644.
9. McDonald, M. B.; Ardo, S.; Lewis, N. S.; Freund, M. S., Use of bipolar membranes for maintaining steady-state pH gradients in membrane-supported, solar-driven water splitting. *ChemSusChem* **2014,** *7* (11), 3021-3027.
10. Vermaas, D. A.; Sassenburg, M.; Smith, W. A., Photo-assisted water splitting with bipolar membrane induced pH gradients for practical solar fuel devices. *Journal of Materials Chemistry A* **2015,** *3* (38), 19556-19562.
11. Peng, S.; Xu, X.; Lu, S.; Sui, P.-C.; Djilali, N.; Xiang, Y., A self-humidifying acidic–alkaline bipolar membrane fuel cell. *Journal of Power Sources* **2015,** *299*, 273-279.
12. Xia, J.; Eigenberger, G.; Strathmann, H.; Nieken, U., Flow battery based on reverse electrodialysis with bipolar membranes: Single cell experiments. **2018,** *565*, 157-168.
13. Dai, J.; Dong, Y.; Gao, P.; Ren, J.; Yu, C.; Hu, H.; Zhu, Y.; Teng, X., A sandwiched bipolar membrane for all vanadium redox flow battery with high coulombic efficiency. *Polymer* **2018,** *140*, 233-239.
14. Tufa, R. A.; Chanda, D.; Ma, M.; Aili, D.; Demissie, T. B.; Vaes, J.; Li, Q.; Liu, S.; Pant, D., Towards highly efficient electrochemical CO2 reduction: Cell designs, membranes and electrocatalysts. *Applied Energy* **2020,** *277*, 115557.
15. Vermaas, D. A.; Smith, W. A., Synergistic Electrochemical CO_2 Reduction and Water Oxidation with a Bipolar Membrane. *ACS Energy Letters* **2016,** *1* (6), 1143-1148.
16. Li, T.; Lees, E. W.; Goldman, M.; Salvatore, D. A.; Weekes, D. M.; Berlinguette, C. P., Electrolytic Conversion of Bicarbonate into CO in a Flow Cell. *Joule* **2019,** *3* (6), 1487-1497.
17. Ma, M.; Kim, S.; Chorkendorff, I.; Seger, B., Role of ion-selective membranes in the carbon balance for CO2 electroreduction via gas diffusion electrode reactor designs. *Chemical Science* **2020,** *11* (33), 8854-8861.
18. van Egmond, W. J.; Saakes, M.; Noor, I.; Porada, S.; Buisman, C. J. N.; Hamelers, H. V. M., Performance of an environmentally benign acid base flow battery at high energy density. **2018,** *42* (4), 1524-1535.
19. Xia, J.; Eigenberger, G.; Strathmann, H.; Nieken, U., Acid-Base Flow Battery, Based on Reverse Electrodialysis with Bi-Polar Membranes: Stack Experiments. **2020,** *8* (1), 99.
20. Culcasi, A.; Gurreri, L.; Zaffora, A.; Cosenza, A.; Tamburini, A.; Micale, G., On the modelling of an Acid/Base Flow Battery: An innovative electrical energy storage device based on pH and salinity gradients. *Applied Energy* **2020,** *277*, 115576.
21. Yan, Z.; Zhu, L.; Li, Y. C.; Wycisk, R. J.; Pintauro, P. N.; Hickner, M. A.; Mallouk, T. E. J. E.; Science, E., The balance of electric field and interfacial catalysis in promoting water dissociation in bipolar membranes. **2018,** *11* (8), 2235-2245.
22. Strathmann, H., *Ion-exchange membrane separation processes*. Elsevier: 2004.
23. Sun, K.; Liu, R.; Chen, Y.; Verlage, E.; Lewis, N. S.; Xiang, C., A Stabilized, Intrinsically Safe, 10% Efficient, Solar-Driven Water-Splitting Cell Incorporating Earth-Abundant Electrocatalysts with Steady-State pH Gradients and Product Separation Enabled by a Bipolar Membrane. **2016,** *6* (13), 1600379.
24. Vermaas, D. A.; Wiegman, S.; Nagaki, T.; Smith, W. A., Ion transport mechanisms in bipolar membranes for (photo)electrochemical water splitting. *Sustainable Energy & Fuels* **2018,** *2* (9), 2006-2015.

25. Blommaert, M. A.; Verdonk, J. A. H.; Blommaert, H. C. B.; Smith, W. A.; Vermaas, D. A., Reduced Ion Crossover in Bipolar Membrane Electrolysis via Increased Current Density, Molecular Size, and Valence. *ACS Applied Energy Materials* **2020,** *3* (6), 5804-5812.
26. Kusoglu, A.; Weber, A. Z., New Insights into Perfluorinated Sulfonic-Acid Ionomers. *Chemical Reviews* **2017,** *117* (3), 987-1104.
27. Bui, J. C.; Digdaya, I.; Xiang, C.; Bell, A. T.; Weber, A. Z., Understanding Multi-Ion Transport Mechanisms in Bipolar Membranes. *ACS Applied Materials & Interfaces* **2020,** *12* (47), 52509-52526.
28. Dekel, D. R.; Amar, M.; Willdorf, S.; Kosa, M.; Dhara, S.; Diesendruck, C. E., Effect of Water on the Stability of Quaternary Ammonium Groups for Anion Exchange Membrane Fuel Cell Applications. *Chemistry of Materials* **2017,** *29* (10), 4425-4431.
29. Varcoe, J. R.; Atanassov, P.; Dekel, D. R.; Herring, A. M.; Hickner, M. A.; Kohl, P. A.; Kucernak, A. R.; Mustain, W. E.; Nijmeijer, K.; Scott, K.; Xu, T.; Zhuang, L., Anion-exchange membranes in electrochemical energy systems. *Energy & Environmental Science* **2014,** *7* (10), 3135-3191.
30. Balster, J.; Srinkantharajah, S.; Sumbharaju, R.; Pünt, I.; Lammertink, R. G. H.; Stamatialis, D. F.; Wessling, M., Tailoring the interface layer of the bipolar membrane. *Journal of Membrane Science* **2010,** *365* (1), 389-398.
31. Mareev, S. A.; Evdochenko, E.; Wessling, M.; Kozaderova, O. A.; Niftaliev, S. I.; Pismenskaya, N. D.; Nikonenko, V. V., A comprehensive mathematical model of water splitting in bipolar membranes: Impact of the spatial distribution of fixed charges and catalyst at bipolar junction. *Journal of Membrane Science* **2020,** *603,* 118010.
32. Oener, S. Z.; Ardo, S.; Boettcher, S. W., Ionic Processes in Water Electrolysis: The Role of Ion-Selective Membranes. *ACS Energy Letters* **2017,** *2* (11), 2625-2634.
33. Strathmann, H.; Krol, J. J.; Rapp, H. J.; Eigenberger, G., Limiting current density and water dissociation in bipolar membranes. *Journal of Membrane Science* **1997,** *125* (1), 123-142.
34. Oener, S. Z.; Twight, L. P.; Lindquist, G. A.; Boettcher, S. W., Thin Cation-Exchange Layers Enable High-Current-Density Bipolar Membrane Electrolyzers via Improved Water Transport. *ACS Energy Letters* **2021,** *6* (1), 1-8.
35. Balster, J.; Sumbharaju, R.; Srikantharajah, S.; Pünt, I.; Stamatialis, D. F.; Jordan, V.; Wessling, M., Asymmetric bipolar membrane: A tool to improve product purity. *Journal of Membrane Science* **2007,** *287* (2), 246-256.
36. Wilhelm, F. G.; Pünt, I.; van der Vegt, N. F. A.; Strathmann, H.; Wessling, M., Asymmetric Bipolar Membranes in Acid−Base Electrodialysis. *Industrial & Engineering Chemistry Research* **2002,** *41* (3), 579-586.
37. Krol, J. J.; Jansink, M.; Wessling, M.; Strathmann, H., Behaviour of bipolar membranes at high current density: Water diffusion limitation. *Separation and Purification Technology* **1998,** *14* (1), 41-52.
38. Yan, Z.; Hitt, J. L.; Zeng, Z.; Hickner, M. A.; Mallouk, T. E., Improving the efficiency of CO2 electrolysis by using a bipolar membrane with a weak-acid cation exchange layer. *Nature Chemistry* **2021,** *13* (1), 33-40.
39. Blommaert, M. A.; Vermaas, D. A.; Izelaar, B.; in 't Veen, B.; Smith, W. A., Electrochemical impedance spectroscopy as a performance indicator of water dissociation in bipolar membranes. *Journal of Materials Chemistry A* **2019,** *7* (32), 19060-19069.

40. Wang, Y.; Chen, K. S.; Mishler, J.; Cho, S. C.; Adroher, X. C., A review of polymer electrolyte membrane fuel cells: Technology, applications, and needs on fundamental research. *Applied Energy* **2011,** *88* (4), 981-1007.
41. Besha, A. T.; Tsehaye, M. T.; Aili, D.; Zhang, W.; Tufa, R. A., Design of Monovalent Ion Selective Membranes for Reducing the Impacts of Multivalent Ions in Reverse Electrodialysis. *Membranes* **2020,** *10* (1), 7.
42. Sahin, S.; Dykstra, J. E.; Zuilhof, H.; Zornitta, R. L.; de Smet, L. C. P. M., Modification of Cation-Exchange Membranes with Polyelectrolyte Multilayers to Tune Ion Selectivity in Capacitive Deionization. *ACS Applied Materials & Interfaces* **2020,** *12* (31), 34746-34754.
43. Tufa, R. A.; Piallat, T.; Hnát, J.; Fontananova, E.; Paidar, M.; Chanda, D.; Curcio, E.; di Profio, G.; Bouzek, K., Salinity gradient power reverse electrodialysis: Cation exchange membrane design based on polypyrrole-chitosan composites for enhanced monovalent selectivity. *Chemical Engineering Journal* **2020,** *380*, 122461.
44. Stenina, I.; Golubenko, D.; Nikonenko, V.; Yaroslavtsev, A., Selectivity of Transport Processes in Ion-Exchange Membranes: Relationship with the Structure and Methods for Its Improvement. **2020,** *21* (15), 5517.
45. Luo, T.; Abdu, S.; Wessling, M., Selectivity of ion exchange membranes: A review. **2018,** *555*, 429-454.
46. Besha, A. T.; Tsehaye, M. T.; Aili, D.; Zhang, W.; Tufa, R. A., Design of monovalent ion selective membranes for reducing the impacts of multivalent ions in reverse electrodialysis. **2020,** *10* (1), 7.
47. Hwang, H. Y.; Koh, H. C.; Rhim, J. W.; Nam, S. Y., Preparation of sulfonated SEBS block copolymer membranes and their permeation properties. **2008,** *233* (1-3), 173-182.
48. Nishimura, M.; Mizutani, Y., Correlation between structure and properties of cation-exchange membranes prepared by the paste method. *Journal of Applied Electrochemistry* **1981,** *11* (2), 165-171.
49. Golubenko, D.; Yaroslavtsev, A., Development of surface-sulfonated graft anion-exchange membranes with monovalent ion selectivity and antifouling properties for electromembrane processes. *Journal of Membrane Science* **2020,** *612*, 118408.
50. Nasef, M. M.; Gürsel, S. A.; Karabelli, D.; Güven, O., Radiation-grafted materials for energy conversion and energy storage applications. *Progress in Polymer Science* **2016,** *63*, 1-41.
51. Nasef, M. M.; Hegazy, E.-S. A., Preparation and applications of ion exchange membranes by radiation-induced graft copolymerization of polar monomers onto non-polar films. *Progress in Polymer Science* **2004,** *29* (6), 499-561.
52. Alabi, A.; AlHajaj, A.; Cseri, L.; Szekely, G.; Budd, P.; Zou, L., Review of nanomaterials-assisted ion exchange membranes for electromembrane desalination. *npj Clean Water* **2018,** *1* (1), 10.
53. Wang, J.; Bai, H.; Zhang, H.; Zhao, L.; Chen, H.; Li, Y., Anhydrous proton exchange membrane of sulfonated poly (ether ether ketone) enabled by polydopamine-modified silica nanoparticles. **2015,** *152*, 443-455.
54. Kreuer, K.-D.; Portale, G., A Critical Revision of the Nano-Morphology of Proton Conducting Ionomers and Polyelectrolytes for Fuel Cell Applications. **2013,** *23* (43), 5390-5397.
55. Mauritz, K. A.; Moore, R. B., State of Understanding of Nafion. *Chemical Reviews* **2004,** *104* (10), 4535-4586.

56. Ciferri, A.; Perico, A., *Ionic interactions in natural and synthetic macromolecules*. John Wiley & Sons: **2012**.
57. Majewski, P. W.; Gopinadhan, M.; Jang, W.-S.; Lutkenhaus, J. L.; Osuji, C. O., Anisotropic Ionic Conductivity in Block Copolymer Membranes by Magnetic Field Alignment. *Journal of the American Chemical Society* **2010,** *132* (49), 17516-17522.
58. Hyun, J.; Doo, G.; Yuk, S.; Lee, D.-H.; Lee, D. W.; Choi, S.; Kwen, J.; Kang, H.; Tenne, R.; Lee, S., Magnetic field-induced through-plane alignment of the proton highway in a proton exchange membrane. **2020,** *3* (5), 4619-4628.
59. Chen, G.; Xu, T.; Liu, J., Irradiation-induced grafting of polyacrylamide onto the sulphonated poly(2,6-dimethyl-1,4-phenylene oxide) (SPPO) films as well as its use as catalytical layer in a bipolar membrane. **2008,** *109* (3), 1447-1453.
60. Assumma, L.; Nguyen, H.-D.; Iojoiu, C.; Lyonnard, S.; Mercier, R.; Espuche, E., Effects of Block Length and Membrane Processing Conditions on the Morphology and Properties of Perfluorosulfonated Poly(arylene ether sulfone) Multiblock Copolymer Membranes for PEMFC. *ACS Applied Materials & Interfaces* **2015,** *7* (25), 13808-13820.
61. Nguyen, H.-D.; Jestin, J.; Porcar, L.; Iojoiu, C.; Lyonnard, S., Aromatic Copolymer/Nafion Blends Outperforming the Corresponding Pristine Ionomers. *ACS Applied Energy Materials* **2018,** *1* (2), 355-367.
62. DeLuca, N. W.; Elabd, Y. A., Nafion®/poly(vinyl alcohol) blends: Effect of composition and annealing temperature on transport properties. *Journal of Membrane Science* **2006,** *282* (1), 217-224.
63. Nguyen, H.-D.; Assumma, L.; Judeinstein, P.; Mercier, R.; Porcar, L.; Jestin, J.; Iojoiu, C.; Lyonnard, S., Controlling Microstructure–Transport Interplay in Highly Phase-Separated Perfluorosulfonated Aromatic Multiblock Ionomers via Molecular Architecture Design. *ACS Applied Materials & Interfaces* **2017,** *9* (2), 1671-1683.
64. Park, J. E.; Kim, J.; Han, J.; Kim, K.; Park, S.; Kim, S.; Park, H. S.; Cho, Y.-H.; Lee, J.-C.; Sung, Y.-E., High-performance proton-exchange membrane water electrolysis using a sulfonated Poly (arylene ether sulfone) membrane and ionomer. **2020**, 118871.
65. Han, J.; Kim, K.; Kim, J.; Kim, S.; Choi, S.-W.; Lee, H.; Kim, J.-j.; Kim, T.-H.; Sung, Y.-E.; Lee, J.-C., Cross-linked highly sulfonated poly(arylene ether sulfone) membranes prepared by in-situ casting and thiol-ene click reaction for fuel cell application. *Journal of Membrane Science* **2019,** *579*, 70-78.
66. Lee, H.; Han, J.; Ahn, S. M.; Jeong, H. Y.; Kim, J.; Kim, H.; Kim, T.-H.; Kim, K.; Lee, J.-C., Simple and Effective Cross-Linking Technology for the Preparation of Cross-Linked Membranes Composed of Highly Sulfonated Poly(ether ether ketone) and Poly(arylene ether sulfone) for Fuel Cell Applications. *ACS Applied Energy Materials* **2020,** *3*, 10495-10505.
67. Qiu, X.; Dong, T.; Ueda, M.; Zhang, X.; Wang, L., Sulfonated reduced graphene oxide as a conductive layer in sulfonated poly (ether ether ketone) nanocomposite membranes. **2017,** *524*, 663-672.
68. Zhang, C.; Yue, X.; Yang, Y.; Lu, N.; Zhang, S.; Wang, G., Thin and methanol-resistant reinforced composite membrane based on semi-crystalline poly (ether ether ketone) for fuel cell applications. **2020,** *450*, 227664.
69. Parnian, M. J.; Rowshanzamir, S.; Prasad, A. K.; Advani, S., High durability sulfonated poly (ether ether ketone)-ceria nanocomposite membranes for proton exchange membrane fuel cell applications. **2018,** *556*, 12-22.

70. Feng, S.; Pang, J.; Yu, X.; Wang, G.; Manthiram, A.; interfaces, High-performance semicrystalline poly (ether ketone)-based proton exchange membrane. **2017,** *9* (29), 24527-24537.
71. Li, C.; Liu, J.; Guan, R.; Zhang, P.; Zhang, Q., Effect of heating and stretching membrane on ionic conductivity of sulfonated poly(phenylene oxide). *Journal of Membrane Science* **2007,** *287* (2), 180-186.
72. Yang, J.; Jiang, H.; Gao, L.; Wang, J.; Ye, N.; Xu, Y.; He, R., Formation and investigation of dual cross-linked high temperature proton exchange membranes based on vinylimidazolium-functionalized poly (2, 6-dimethyl-1, 4-phenylene oxide) and polystyrene. **2018,** *9* (45), 5462-5469.
73. Li, J.; Yuan, X.; Liu, S.; He, Z.; Zhou, Z.; Li, A.; interfaces, A low-cost and high-performance sulfonated polyimide proton-conductive membrane for vanadium redox flow/static batteries. **2017,** *9* (38), 32643-32651.
74. Xia, Y.; Liu, B.; Wang, Y., Effects of covalent bond interactions on properties of polyimide grafting sulfonated polyvinyl alcohol proton exchange membrane for vanadium redox flow battery applications. **2019,** *433*, 126680.
75. Pu, Y.; Zhu, S.; Wang, P.; Zhou, Y.; Yang, P.; Xuan, S.; Zhang, Y.; Zhang, H., Novel branched sulfonated polyimide/molybdenum disulfide nanosheets composite membrane for vanadium redox flow battery application. **2018,** *448*, 186-202.
76. Klose, C.; Saatkamp, T.; Münchinger, A.; Bohn, L.; Titvinidze, G.; Breitwieser, M.; Kreuer, K.-D.; Vierrath, S., All-Hydrocarbon MEA for PEM Water Electrolysis Combining Low Hydrogen Crossover and High Efficiency. **2020,** *10* (14), 1903995.
77. Li, Q.; Jensen, J. O.; Savinell, R. F.; Bjerrum, N. J., High temperature proton exchange membranes based on polybenzimidazoles for fuel cells. *Progress in Polymer Science* **2009,** *34* (5), 449-477.
78. Ding, L.; Song, X.; Wang, L.; Zhao, Z.; He, G., Preparation of dense polybenzimidazole proton exchange membranes with different basicity and flexibility for vanadium redox flow battery applications. **2018,** *292*, 10-19.
79. Cai, Y.; Yue, Z.; Teng, X.; Xu, S., Radiation grafting graphene oxide reinforced polybenzimidazole membrane with a sandwich structure for high temperature proton exchange membrane fuel cells in anhydrous atmosphere. **2018,** *103*, 207-213.
80. Shin, D. W.; Guiver, M. D.; Lee, Y. M., Hydrocarbon-Based Polymer Electrolyte Membranes: Importance of Morphology on Ion Transport and Membrane Stability. *Chemical Reviews* **2017,** *117* (6), 4759-4805.
81. Titvinidze, G.; Kreuer, K.-D.; Schuster, M.; de Araujo, C. C.; Melchior, J. P.; Meyer, W. H., Proton Conducting Phase-Separated Multiblock Copolymers with Sulfonated Poly(phenylene sulfone) Blocks for Electrochemical Applications: Preparation, Morphology, Hydration Behavior, and Transport. **2012,** *22* (21), 4456-4470.
82. Schuster, M.; Kreuer, K.-D.; Andersen, H. T.; Maier, J., Sulfonated Poly(phenylene sulfone) Polymers as Hydrolytically and Thermooxidatively Stable Proton Conducting Ionomers. *Macromolecules* **2007,** *40* (3), 598-607.
83. Hohenadel, A.; Powers, D.; Wycisk, R.; Adamski, M.; Pintauro, P.; Holdcroft, S., Electrochemical Characterization of Hydrocarbon Bipolar Membranes with Varying Junction Morphology. *ACS Applied Energy Materials* **2019,** *2* (9), 6817-6824.

84. Kim, D. S.; Kim, Y. S.; Guiver, M. D.; Ding, J.; Pivovar, B. S., Highly fluorinated comb-shaped copolymer as proton exchange membranes (PEMs): Fuel cell performance. *Journal of Power Sources* **2008,** *182* (1), 100-105.
85. Liu, B.; Robertson, G. P.; Kim, D.-S.; Guiver, M. D.; Hu, W.; Jiang, Z., Aromatic Poly(ether ketone)s with Pendant Sulfonic Acid Phenyl Groups Prepared by a Mild Sulfonation Method for Proton Exchange Membranes. *Macromolecules* **2007,** *40* (6), 1934-1944.
86. Vogel, C.; Meier-Haack, J., Preparation of ion-exchange materials and membranes. *Desalination* **2014,** *342*, 156-174.
87. Guiver, M. D.; Robertson, G. P.; Yoshikawa, M.; Tam, C. M., Functionalized polysulfones: Methods for chemical modification and membrane applications. ACS Publications: **2000**, 137-161.
88. Khomein, P.; Ketelaars, W.; Lap, T.; Liu, G., Sulfonated aromatic polymer as a future proton exchange membrane: A review of sulfonation and crosslinking methods. *Renewable and Sustainable Energy Reviews* **2021**, *137*, 110471.
89. Zhang, Z.; Wu, L.; Xu, T., Novel aromatic proton-exchange polyelectrolytes via polyacylation of pre-sulfonated monomers. *Journal of Materials Chemistry* **2012,** *22* (28), 13996-14000.
90. Zhang, Z.; Xu, T., Poly(ether ketone)s bearing pendent sulfonate groups via copolyacylation of a sulfonated monomer and isomeric AB-type comonomers. *Journal of Polymer Science, Part A: Polymer Chemistry* **2014,** *52* (2), 200-207.
91. Zhao, J.; Guo, L.; Wang, J., Synthesis of cation exchange membranes based on sulfonated polyether sulfone with different sulfonation degrees. *Journal of Membrane Science* **2018,** *563*, 957-968.
92. Cui, M.; Zhang, Z.; Yuan, T.; Yang, H.; Wu, L.; Bakangura, E.; Xu, T., Proton-conducting membranes based on side-chain-type sulfonated poly(ether ketone/ether benzimidazole)s via one-pot condensation. *Journal of Membrane Science* **2014,** *465*, 100-106.
93. Si, K.; Dong, D.; Wycisk, R.; Litt, M., Synthesis and characterization of poly(para-phenylene disulfonic acid), its copolymers and their n-alkylbenzene grafts as proton exchange membranes: high conductivity at low relative humidity. *Journal of Materials Chemistry* **2012,** *22* (39), 20907-20917.
94. Chen, S.; Hara, R.; Chen, K.; Zhang, X.; Endo, N.; Higa, M.; Okamoto, K.-i.; Wang, L., Poly(phenylene) block copolymers bearing tri-sulfonated aromatic pendant groups for polymer electrolyte fuel cell applications. *Journal of Materials Chemistry A* **2013,** *1* (28), 8178-8189.
95. Wang, L.; Liu, M.; Zhao, J.; Lei, Y.; Li, N., Comb-shaped sulfonated poly(ether ether ketone) as a cation exchange membrane for electrodialysis in acid recovery. *Journal of Materials Chemistry A* **2018,** *6* (45), 22940-22950.
96. Li, N.; Wang, C.; Lee, S. Y.; Park, C. H.; Lee, Y. M.; Guiver, M. D., Enhancement of Proton Transport by Nanochannels in Comb-Shaped Copoly(arylene ether sulfone)s. **2011,** *50* (39), 9158-9161.
97. Takamuku, S.; Wohlfarth, A.; Manhart, A.; Räder, P.; Jannasch, P., Hypersulfonated polyelectrolytes: preparation, stability and conductivity. *Polymer Chemistry* **2015,** *6* (8), 1267-1274.
98. Miller, H. A.; Bouzek, K.; Hnat, J.; Loos, S.; Bernäcker, C. I.; Weißgärber, T.; Röntzsch, L.; Meier-Haack, J., Green hydrogen from anion exchange membrane water

electrolysis: a review of recent developments in critical materials and operating conditions. *Sustainable Energy & Fuels* **2020,** *4* (5), 2114-2133.
99. Noh, S.; Jeon, J. Y.; Adhikari, S.; Kim, Y. S.; Bae, C., Molecular Engineering of Hydroxide Conducting Polymers for Anion Exchange Membranes in Electrochemical Energy Conversion Technology. *Accounts of Chemical Research* **2019,** *52* (9), 2745-2755.
100. Merle, G.; Wessling, M.; Nijmeijer, K., Anion exchange membranes for alkaline fuel cells: A review. *Journal of Membrane Science* **2011,** *377* (1), 1-35.
101. Li, D.; Matanovic, I.; Lee, A. S.; Park, E. J.; Fujimoto, C.; Chung, H. T.; Kim, Y. S., Phenyl Oxidation Impacts the Durability of Alkaline Membrane Water Electrolyzer. *ACS Applied Materials & Interfaces* **2019,** *11* (10), 9696-9701.
102. Liu, L.; Chu, X.; Liao, J.; Huang, Y.; Li, Y.; Ge, Z.; Hickner, M. A.; Li, N.; Science, E., Tuning the properties of poly (2, 6-dimethyl-1, 4-phenylene oxide) anion exchange membranes and their performance in H 2/O2 fuel cells. **2018,** *11* (2), 435-446.
103. Mahmoud, A. M. A.; Miyatake, K., Optimization of the pendant chain length in partially fluorinated aromatic anion exchange membranes for alkaline fuel cells. **2018,** *6* (29), 14400-14409.
104. Pham, T. H.; Olsson, J. S.; Jannasch, P., Poly (arylene alkylene) s with pendant N-spirocyclic quaternary ammonium cations for anion exchange membranes. **2018,** *6* (34), 16537-16547.
105. Chen, N.; Long, C.; Li, Y.; Lu, C.; Zhu, H.; interfaces, Ultrastable and high ion-conducting polyelectrolyte based on six-membered N-spirocyclic ammonium for hydroxide exchange membrane fuel cell applications. **2018,** *10* (18), 15720-15732.
106. Pham, T. H.; Olsson, J. S.; Jannasch, P., N-spirocyclic quaternary ammonium ionenes for anion-exchange membranes. **2017,** *139* (8), 2888-2891.
107. Womble, C. T.; Coates, G. W.; Matyjaszewski, K.; Noonan, K., Tetrakis (dialkylamino) phosphonium polyelectrolytes prepared by reversible addition–fragmentation chain transfer polymerization. **2016,** *5* (2), 253-257.
108. Womble, C. T.; Kang, J.; Hugar, K. M.; Coates, G. W.; Bernhard, S.; Noonan, K., Rapid analysis of tetrakis (dialkylamino) phosphonium stability in alkaline media. **2017,** *36* (20), 4038-4046.
109. Yang, C.; Liu, L.; Han, X.; Huang, Z.; Dong, J.; Li, N., Highly anion conductive, alkyl-chain-grafted copolymers as anion exchange membranes for operable alkaline H 2/O 2 fuel cells. **2017,** *5* (21), 10301-10310.
110. Liu, D.; Xu, M.; Fang, M.; Chen, J.; Wang, L., Branched comb-shaped poly (arylene ether sulfone) s containing flexible alkyl imidazolium side chains as anion exchange membranes. **2018,** *6* (23), 10879-10890.
111. Wright, A. G.; Fan, J.; Britton, B.; Weissbach, T.; Lee, H.-F.; Kitching, E. A.; Peckham, T. J.; Holdcroft, S. J. E.; Science, E., Hexamethyl-p-terphenyl poly (benzimidazolium): a universal hydroxide-conducting polymer for energy conversion devices. **2016,** *9* (6), 2130-2142.
112. Zhu, Y.; He, Y.; Ge, X.; Liang, X.; Shehzad, M. A.; Hu, M.; Liu, Y.; Wu, L.; Xu, T. J. J. o. M. C. A., A benzyltetramethylimidazolium-based membrane with exceptional alkaline stability in fuel cells: role of its structure in alkaline stability. **2018,** *6* (2), 527-534.
113. Gu, S.; Wang, J.; Kaspar, R. B.; Fang, Q.; Zhang, B.; Coughlin, E. B.; Yan, Y., Permethyl cobaltocenium (Cp* 2 Co+) as an ultra-stable cation for polymer hydroxide-exchange membranes. **2015,** *5*, 11668.

114. Kwasny, M. T.; Tew, G., Expanding metal cation options in polymeric anion exchange membranes. **2017,** *5* (4), 1400-1405.
115. Kwasny, M. T.; Zhu, L.; Hickner, M. A.; Tew, G., Thermodynamics of counterion release is critical for anion exchange membrane conductivity. **2018,** *140* (25), 7961-7969.
116. Carter, Blaine M.; Keller, L.; Wessling, M.; Miller, D. J., Preparation and characterization of crosslinked poly(vinylimidazolium) anion exchange membranes for artificial photosynthesis. *Journal of Materials Chemistry A* **2019,** *7* (41), 23818-23829.
117. Dischinger, S. M.; Gupta, S.; Carter, B. M.; Miller, D. J., Transport of Neutral and Charged Solutes in Imidazolium-Functionalized Poly(phenylene oxide) Membranes for Artificial Photosynthesis. *Industrial & Engineering Chemistry Research* **2020,** *59* (12), 5257-5266.
118. Hugar, K. M.; Kostalik IV, H. A.; Coates, G., Imidazolium cations with exceptional alkaline stability: a systematic study of structure–stability relationships. **2015,** *137* (27), 8730-8737.
119. Fan, J.; Wright, A. G.; Britton, B.; Weissbach, T.; Skalski, T. J.; Ward, J.; Peckham, T. J.; Holdcroft, S., Cationic polyelectrolytes, stable in 10 M KOHaq at 100° C. **2017,** *6* (10), 1089-1093.
120. You, W.; Hugar, K. M.; Coates, G., Synthesis of alkaline anion exchange membranes with chemically stable imidazolium cations: Unexpected cross-linked macrocycles from ring-fused ROMP monomers. **2018,** *51* (8), 3212-3218.
121. Hnát, J.; Plevová, M.; Žitka, J.; Paidar, M.; Bouzek, K., Anion-selective materials with 1, 4-diazabicyclo [2.2. 2] octane functional groups for advanced alkaline water electrolysis. **2017,** *248*, 547-555.
122. You, W.; Padgett, E.; MacMillan, S. N.; Muller, D. A.; Coates, G. W., Highly conductive and chemically stable alkaline anion exchange membranes via ROMP of *trans*-cyclooctene derivatives. *PNAS* **2019,** *116* (20), 9729-9734.
123. Li, Y.; Liu, Y.; Savage, A. M.; Beyer, F. L.; Seifert, S.; Herring, A. M.; Knauss, D. M. J. M., Polyethylene-based block copolymers for anion exchange membranes. **2015,** *48* (18), 6523-6533.
124. Walker, R.; Conrad, R. M.; Grubbs, R. H. J. M., The living ROMP of trans-cyclooctene. **2009,** *42* (3), 599-605.
125. Dang, H.-S.; Jannasch, P., Exploring Different Cationic Alkyl Side Chain Designs for Enhanced Alkaline Stability and Hydroxide Ion Conductivity of Anion-Exchange Membranes. *Macromolecules* **2015,** *48* (16), 5742-5751.
126. Lee, W.-H.; Kim, Y. S.; Bae, C. J. A. M. L., Robust hydroxide ion conducting poly (biphenyl alkylene) s for alkaline fuel cell membranes. **2015,** *4* (8), 814-818.
127. Lee, W.-H.; Park, E. J.; Han, J.; Shin, D. W.; Kim, Y. S.; Bae, C., Poly(terphenylene) Anion Exchange Membranes: The Effect of Backbone Structure on Morphology and Membrane Property. *ACS Macro Letters* **2017,** *6* (5), 566-570.
128. Aili, D.; Hansen, M. K.; Renzaho, R. F.; Li, Q.; Christensen, E.; Jensen, J. O.; Bjerrum, N. J., Heterogeneous anion conducting membranes based on linear and crosslinked KOH doped polybenzimidazole for alkaline water electrolysis. *Journal of Membrane Science* **2013,** *447*, 424-432.
129. Konovalova, A.; Kim, H.; Kim, S.; Lim, A.; Park, H. S.; Kraglund, M. R.; Aili, D.; Jang, J. H.; Kim, H.-J.; Henkensmeier, D., Blend membranes of polybenzimidazole and an anion exchange ionomer (FAA3) for alkaline water electrolysis: improved alkaline stability and conductivity. **2018,** *564*, 653-662.

130. Kraglund, M. R.; Carmo, M.; Schiller, G.; Ansar, S. A.; Aili, D.; Christensen, E.; Jensen, J. O. J. E.; Science, E., Ion-solvating membranes as a new approach towards high rate alkaline electrolyzers. **2019,** *12* (11), 3313-3318.
131. Aili, D.; Yang, J.; Jankova, K.; Henkensmeier, D.; Li, Q., From polybenzimidazoles to polybenzimidazoliums and polybenzimidazolides. **2020,** *8* (26), 12854-12886.
132. Pham, T. H.; Olsson, J. S.; Jannasch, P., N-Spirocyclic Quaternary Ammonium Ionenes for Anion-Exchange Membranes. *Journal of the American Chemical Society* **2017,** *139* (8), 2888-2891.
133. Arges, C. G.; Zhang, L., Anion Exchange Membranes' Evolution toward High Hydroxide Ion Conductivity and Alkaline Resiliency. *ACS Applied Energy Materials* **2018,** *1* (7), 2991-3012.
134. Hren, M.; Bozic, M.; Fakin, D.; Stana-Kleinschek, K.; Gorgieva, S., Alkaline membrane fuel cells: Anion exchange membranes and fuels. *Sustainable Energy & Fuels* **2021,** *5*, 604-637.
135. Mafé, S.; Ramírez, P., Electrochemical characterization of polymer ion-exchange bipolar membranes. **1997,** *48* (7), 234-250.
136. Kole, S.; Venugopalan, G.; Bhattacharya, D.; Zhang, L.; Cheng, J. H.; Pivovar, B.; Arges, C. G., Bipolar membrane polarization behavior with systematically varied interfacial areas in the junction region. **2021,** *9*, 2223-2238.
137. McDonald, M. B.; Freund, M. S., Graphene Oxide as a Water Dissociation Catalyst in the Bipolar Membrane Interfacial Layer. *ACS Applied Materials & Interfaces* **2014,** *6* (16), 13790-13797.
138. Chabi, S.; Wright, A. G.; Holdcroft, S.; Freund, M. S., Transparent Bipolar Membrane for Water Splitting Applications. *ACS Applied Materials & Interfaces* **2017,** *9* (32), 26749-26755.
139. Hodgdon, R. B.; Alexander, S. S., Novel bipolar membranes and process of manufacture. Google Patents: **1989**.
140. Frilette, V. J., Preparation and Characterization of Bipolar Ion Exchange Membranes. *The Journal of Physical Chemistry* **1956,** *60* (4), 435-439.
141. Dege, G. J.; Liu, K.-J., Method of making single film, high performance bipolar membrane. Google Patents: **1979**.
142. Shen, C.; Wycisk, R.; Pintauro, P. N., High performance electrospun bipolar membrane with a 3D junction. *Energy & Environmental Science* **2017,** *10* (6), 1435-1442.
143. Yan, Z.; Zhu, L.; Li, Y. C.; Wycisk, R. J.; Pintauro, P. N.; Hickner, M. A.; Mallouk, T. E., The balance of electric field and interfacial catalysis in promoting water dissociation in bipolar membranes. *Energy and Environmental Science* **2018,** *11* (8), 2235-2245.
144. Zhang, W.; Miao, M.; Pan, J.; Sotto, A.; Shen, J.; Gao, C.; Van der Bruggen, B. J. A. S. C.; Engineering, Process economic evaluation of resource valorization of seawater concentrate by membrane technology. **2017,** *5* (7), 5820-5830.
145. Manohar, M.; Shahi, V. K., Graphene Oxide–Polyaniline as a Water Dissociation Catalyst in the Interfacial Layer of Bipolar Membrane for Energy-Saving Production of Carboxylic Acids from Carboxylates by Electrodialysis. *ACS Sustainable Chemistry & Engineering* **2018,** *6* (3), 3463-3471.
146. Simons, R., A novel method for preparing bipolar membranes. *Electrochimica Acta* **1986,** *31* (9), 1175-1177.

147. Simons, R., Preparation of a high performance bipolar membrane. *Journal of Membrane Science* **1993,** *78* (1), 13-23.
148. Kim, B. S.; Park, S. C.; Kim, D.-H.; Moon, G. H.; Oh, J. G.; Jang, J.; Kang, M.-S.; Yoon, K. B.; Kang, Y. S., Bipolar Membranes to Promote Formation of Tight Ice-Like Water for Efficient and Sustainable Water Splitting. **2020,** *16* (41), 2002641.
149. Manohar, M.; Shahi, V.; Engineering, Graphene Oxide–Polyaniline as a Water Dissociation Catalyst in the Interfacial Layer of Bipolar Membrane for Energy-Saving Production of Carboxylic Acids from Carboxylates by Electrodialysis. **2018,** *6* (3), 3463-3471.
150. McDonald, M. B.; Freund, M.; interfaces, Graphene oxide as a water dissociation catalyst in the bipolar membrane interfacial layer. **2014,** *6* (16), 13790-13797.
151. Sheldeshov, N.; Zabolotskii, V.; Pis-menskaya, N.; Gnusin, N.P., Catalysis of water dissociation by the phosphoric-acid groups of an MB-3 bipolar membrane. *Sov. Electrochem. (Engl. Transl.)* **1986,** *22* (6).
152. Strathmann, H.; Rapp, H. J.; Bauer, B.; Bell, C. M., Theoretical and practical aspects of preparing bipolar membranes. *Desalination* **1993,** *90* (1), 303-323.
153. Simons, R. G., High performance bipolar membranes. Google Patents: **1993**.
154. Posar, F.; Ricciardi, M., Process for the manufacture of a bipolar membrane and process for the manufacture of an aqueous alkali metal hydroxide solution. Google Patents: **1995**.
155. Kang, M.-S.; Choi, Y.-J.; Moon, S.-H., Effects of inorganic substances on water splitting in ion-exchange membranes: II. Optimal contents of inorganic substances in preparing bipolar membranes. *Journal of Colloid and Interface Science* **2004,** *273* (2), 533-539.
156. Bauer, B.; Gerner, F. J.; Strathmann, H., Development of bipolar membranes. *Desalination* **1988,** *68* (2), 279-292.
157. Wakamatsu, Y.; Matsumoto, H.; Minagawa, M.; Tanioka, A., Effect of ion-exchange nanofiber fabrics on water splitting in bipolar membrane. *Journal of Colloid and Interface Science* **2006,** *300* (1), 442-445.
158. Melnikov, S. S.; Sheldeshov, N. V.; Zabolotskii, V. I., Theoretical and experimental study of current–voltage characteristics of asymmetric bipolar membranes. *Desalination and Water Treatment* **2018,** *123*, 1-13.
159. Kovalchuk, V. I.; Zholkovskij, E. K.; Aksenenko, E. V.; Gonzalez-Caballero, F.; Dukhin, S. S., Ionic transport across bipolar membrane and adjacent Nernst layers. *Journal of Membrane Science* **2006,** *284* (1), 255-266.
160. Martinez, R. J.; Farrell, J., Quantifying Electric Field Enhancement of Water Dissociation Rates in Bipolar Membranes. *Industrial & Engineering Chemistry Research* **2019,** *58* (2), 782-789.
161. Conroy, D. T.; Craster, R. V.; Matar, O. K.; Cheng, L. J.; Chang, H. C., Nonequilibrium hysteresis and Wien effect water dissociation at a bipolar membrane. *Physical Review E* **2012,** *86* (5), 056104.
162. Yokoyama, Y.; Tanioka, A.; Miyasaka, K., Preparation of a single bipolar membrane by plasma-induced graft polymerization. *Journal of Membrane Science* **1989,** *43* (2), 165-175.
163. De Körösy, F.; Zeigerson, E., Bipolar membranes made of a single polyolephine sheet. **1971,** *9* (4), 483-497.
164. Lee, L. T.; Dege, G. J.; Liu, K.-J., High performance, quality controlled bipolar membrane. Google Patents: **1977**.

165. Abdu, S.; Sricharoen, K.; Wong, J. E.; Muljadi, E. S.; Melin, T.; Wessling, M., Catalytic Polyelectrolyte Multilayers at the Bipolar Membrane Interface. *ACS Applied Materials & Interfaces* **2013,** *5* (21), 10445-10455.
166. Pan, J.; Hou, L.; Wang, Q.; He, Y.; Wu, L.; Mondal, A. N.; Xu, T., Preparation of bipolar membranes by electrospinning. *Materials Chemistry and Physics* **2017,** *186*, 484-491.
167. Lebrun, L.; Da Silva, E.; Pourcelly, G.; Métayer, M., Elaboration and characterisation of ion-exchange films used in the fabrication of bipolar membranes. *Journal of Membrane Science* **2003,** *227* (1), 95-111.
168. Chen, Y.; Martínez, R. J.; Gervasio, D.; Baygents, J. C.; Farrell, J., Water splitting promoted by electronically conducting interlayer material in bipolar membranes. *Journal of Applied Electrochemistry* **2020,** *50* (1), 33-40.
169. McClure, J. P.; Grew, K. N.; Chu, D., Experimental Development of Alkaline and Acid-Alkaline Bipolar Membrane Electrolytes. *ECS Transactions* **2015,** *69* (18), 35-44.
170. Dong, Z.; Kennedy, S. J.; Wu, Y., Electrospinning materials for energy-related applications and devices. *Journal of Power Sources* **2011,** *196* (11), 4886-4904.
171. Thavasi, V.; Singh, G.; Ramakrishna, S., Electrospun nanofibers in energy and environmental applications. *Energy & Environmental Science* **2008,** *1* (2), 205-221.
172. Fu, R.; Xu, T.; Yang, W.; Pan, Z., Preparation of a mono-sheet bipolar membrane by simultaneous irradiation grafting polymerization of acrylic acid and chloromethylstyrene. **2003,** *90* (2), 572-576.
173. Hsueh, C.-L.; Peng, Y.-J.; Wang, C.-C.; Chen, C.-Y., Bipolar membrane prepared by grafting and plasma polymerization. *Journal of Membrane Science* **2003,** *219* (1), 1-13.
174. Moussaoui, R. E.; Pourcelly, G.; Maeck, M.; Hurwitz, H. D.; Gavach, C., Co-ion leakage through bipolar membranes Influence on I–V responses and water-splitting efficiency. *Journal of Membrane Science* **1994,** *90* (3), 283-292.

For Table of Contents Only